Spatiotemporal dynamics of SETD5-containing NCoR-HDAC3 complex determines enhancer activation for adipogenesis

Yoshihiro Matsumura
Division of Metabolic Medicine, RCAST, The University of Tokyo
Ryo Ito
Tohoku University Graduate School of Medicine
Ayumu Yajima
The University of Tokyo
Rei Yamaguchi
Tohoku University Graduate School of Medicine
Kenta Magoori
The University of Tokyo
Toshiya Tanaka
The University of Tokyo https://orcid.org/0000-0003-1224-7898
Takeshi Kawamura
The University of Tokyo
Hiroyuki Hirakawa
The University of Tokyo
Hitomi Fujihashi
The University of Tokyo
Yohei Abe
The University of Tokyo
Ryo Nakaki
The University of Tokyo
Aoi Uchida
Division of Metabolic Medicine, RCAST, The University of Tokyo
Shogo Yamamoto
Research Center for Advanced Science and Technology, The University of Tokyo
https://orcid.org/0000-0002-5564-2567
Satoshi Ota
The University of Tokyo
Shuichi Tsutsumi
University of Tokyo

Shin-ichi Inoue
Tohoku University
Hiroshi Kimura
Tokyo Institute of Technology https://orcid.org/0000-0003-0854-083X
Yoichiro Wada
University of Tokyo
Takeshi Inagaki
The University of Tokyo
Tatsuhiko Kodama
University of Tokyo
Timothy Osborne
Institute for Fundamental Biomedical Research
Hiroyuki Aburatani
University of Tokyo https://orcid.org/0000-0003-0438-1544
Koichi Node
Saga University https://orcid.org/0000-0002-2534-0939
Juro Sakai (jmsakai-tky@umin.ac.jp)
Division of Metabolic Medicine, RCAST, The University of Tokyo

---

Article

Keywords: adipogenesis, cell-type specific gene expression

Posted Date: February 25th, 2021

DOI: https://doi.org/10.21203/rs.3.rs-250361/v1

Version of Record: A version of this preprint was published at Nature Communications on December 1st, 2021. See the published version at https://doi.org/10.1038/s41467-021-27321-5.

Spatiotemporal dynamics of SETD5-containing NCoR-HDAC3 complex determines enhancer activation for adipogenesis

Yoshihiro Matsumura,[1,12,*] Ryo Ito,[10,12] Ayumu Yajima,[1,6,12] Rei Yamaguchi,[10] Kenta Magoori,[1] Toshiya Tanaka,[2] Takeshi Kawamura,[4] Hiroyuki Hirakawa,[1,5] Hitomi Fujihashi,[1] Yohei Abe,[1] Aoi Uchida,[1] Ryo Nakaki,[3,7] Shogo Yamamoto,[3] Satoshi Ota, [3] Shuichi Tsutsumi,[3] Shin-ichi Inoue,[10] Hiroshi Kimura,[8] Youichiro Wada,[4] Tatsuhiko Kodama,[2] Takeshi Inagaki,[1,9] Timothy F. Osborne,[11] Hiroyuki Aburatani,[3] Koichi Node,[6] and Juro Sakai,[1,10,*]

[1]Division of Metabolic Medicine

[2]Department of Nuclear Receptor Medicine, Laboratories for Systems Biology and Medicine

[3]Genome Science Division, Research Center for Advanced Science and Technology, The University of Tokyo, Tokyo 153-8904, Japan

[4]Isotope Science Center, The University of Tokyo, Tokyo 113-0032, Japan

[5]Department of Physiology and Cell Biology, Tokyo Medical and Dental University (TMDU), Graduate School, Tokyo 113-8510, Japan

[6]Department of Cardiovascular Medicine, Saga University, Saga 849-8501, Japan

[7]Rhelixa Inc., Tokyo 101-0061, Japan

[8]Cell Biology Center, Institute of Innovative Research, Tokyo Institute of Technology, Yokohama 226-8503, Japan

[9]Laboratory of Epigenetics and Metabolism, Institute for Molecular and Cellular Regulation, Gunma University, Gunma 371-8512, Japan

[10]Division of Molecular Physiology and Metabolism, Tohoku University Graduate School of Medicine, Sendai 980-8574, Japan

[11]Institute for Fundamental Biomedical Research, Johns Hopkins All Children's Hospital, and Medicine in the Division of Endocrinology, Diabetes and Metabolism of the Johns Hopkins University School of Medicine, 600 Fifth Street S. St. Petersburg, FL 33701, USA.

[12]These authors contributed equally.

*Correspondence: matsumura-y@lsbm.org (Y.M.), jmsakai@med.tohoku.ac.jp (J.S.)

Abstract

Enhancer activation is essential for cell-type specific gene expression during cellular differentiation, however, how enhancers transition from a hypoacetylated "primed" state to a hyperacetylated-active state is incompletely understood. Here, we show SET domain-containing 5 (SETD5) forms a complex with NCoR-HDAC3 co-repressor that prevents histone acetylation of enhancers for two master adipogenic regulatory genes *Cebpa* and *Pparg* early during adipogenesis. The loss of SETD5 from the complex is followed by enhancer hyperacetylation. SETD5 protein levels were transiently increased and rapidly degraded prior to enhancer activation providing a mechanism for the loss of SETD5 during the transition. We show that induction of the CDC20 co-activator of the ubiquitin ligase leads to APC/C mediated degradation of SETD5 during the transition and this operates as a molecular switch that facilitates adipogenesis.

Introduction

Cell-type specific gene expression is spatially and temporally regulated by DNA cis-regulatory elements called enhancers that can be located at varying locations relative to their target genes ranging from a few hundred to mega-base distances. Enhancers interact with proximal promoter elements via long-range chromatin looping events mediated by transcription factors that are recruited to specific binding sites located within both enhancers and proximal promoters through systematic interactions with non-DNA binding transcriptional coregulatory and chromatin modifying complexes and the combined action results in regulated augmentation of basal transcription levels [1]. Enhancers are selected and activated in a cell-type specific manner during development and in response to specific stimuli. Enhancer selection and activation involve binding of lineage-determining transcription factors to their recognition motif combined with local nucleosome remodeling [2, 3, 4].

The transcription factor complexes that bind to enhancer and promoter motifs contain histone modification enzymes that mark enhancer and proximal promoter regions with specific histone modification signatures. For example, enhancer chromatin displays an enrichment for histone H3 lysine 4 mono- methylation (H3K4me1) and low levels of H3K4 tri-methylation (H3K4me3) compared with promoters which show enrichment for

H3K4me3 [5]. Enhancers can be classified as poised, primed, or active, defined by a combination of unique histone modifications which can be interconverted [6] (also reviewed in [4]). Poised enhancers are marked with H3 lysine 27 tri-methylation (H3K27me3), a repressive epigenetic mark (see also Fig. 1a). Poised enhancers are inefficient at driving gene expression, however, they are converted to active enhancers during differentiation through the loss of repressive H3K27me3 and a gain of the activating H3 lysine 27 acetylation (H3K27ac) mark. Prior to activation, enhancers can also exist in a primed state. Primed enhancers are characterized by the presence of H3K4me1 but they lack both repressive H3K27me3 and active H3K27ac. Additional cues such as signal dependent stimuli result in recruitment of additional transcription factors, and the eventual recruitment of co-activators leading to enhancer activation. Active enhancers simultaneously contain both H3K4me1 and H3K27ac.

The acetylation state of a given chromatin locus is controlled by two classes of antagonizing histone modifying enzymes, histone acetyltransferases (HATs; e.g. CBP and p300) [5, 7] and deacetylases (HDACs), which are components of co-repressors such as nuclear receptor co-repressors (NCoRs) and SMRT [8, 9, 10]. HATs facilitate H3K27 acetylation [5, 7], whereas HDAC-containing complexes remove H3K27 acetylation [11, 12]. Because H3K27ac determines whether an enhancer is primed or active [6], the relative

recruitment ratio of HATs "writers" and HDACs "erasers" to enhancer chromatin is likely a key determinant for acetylation status. However, molecular mechanisms that keep enhancers in a primed state are not fully understood.

The differentiation program converting preadipocytes into adipocytes has been well studied, especially in cultured mouse 3T3-L1 cell lines [13, 14]. Growth-arrested 3T3-L1 preadipocytes synchronously reenter the cell cycle and undergo two rounds of mitotic clonal expansion followed by acquisition of the mature adipocyte phenotype [15]. This process, called adipogenesis, is orchestrated by a cascade of sequentially acting cell cycle proteins, transcription factors, and chromatin modifiers that shape the differentiation through the symphonic interplay of hormones and other signaling pathways (reviewed in [13, 16, 17, 18]). During this period, there is a rapid and transient induction of transcription factors CCAAT/enhancer-binding protein β (C/EBPβ) and C/EBPδ (2-4 hrs), that are recruited to binding sites of C/EBPα and PPARγ gene enhancers (4-24 hrs), yet they remain transcriptionally silent. After 36 hrs, when the first round of mitosis is completed during clonal expansion, enhancers are transformed to the active state which is followed by gene activation (36 hrs and later) [19] [15] (also reviewed in [18]). These two master regulators, C/EBPα and PPARγ, together orchestrate the global changes in gene expression that cause the acquisition of the mature fat-laden adipocyte phenotype as the second round of mitosis

is completed [15, 20, 21].

The anaphase-promoting complex/cyclosome (APC/C) is an evolutionarily conserved multi-subunit ubiquitin ligase that controls cell cycle progression through proteasomal degradation of key cell cycle regulatory targets [22]. Recent studies have revealed it also plays a role in postmitotic cellular responses to developmental signals through transcriptional regulation of genes by directly targeting various cell type-specific transcription factors and their regulators for degradation. The catalytic core of APC/C is comprised of the cullin subunit ANAPC2 and RING domain subunit ANAPC11. CDC20 and CDH1, two structurally homologous accessory subunits, are referred to as "APC/C coactivators" and mediate substrate recognition and stimulation of the ubiquitin ligase activity of APC/C. CDC20 binds and activates APC/C in M phase to trigger chromatid separation and mitotic exit (reviewed in [23], see also the schematic illustration in Supplementary Fig. 3c).

Our previous genome-wide search for epigenetic regulators involved in adipogenesis revealed several genes encoding SET domain-containing proteins [21]. Among them, SETD5 is a potential histone methyltransferase whose gene expression declines during the first 48 hrs of adipogenesis [21]. Recent genetic studies reported loss-of function mutations in *SETD5* in patients with intellectual disability [24, 25, 26] and studies in *Setd5*

mutant mice suggested roles of SETD5 in neuronal development, however, whether it actually contains histone methyltransferase activity has been controversial and could be context dependent [27, 28, 29, 30].

In this study, we show that SETD5 performs a structural role in formation of a complex with NCoR-HDAC3 repressor complex to keep enhancers hypoacetylated and in a "primed" state by restricting recruitment of HATs to the enhancers of *Cebpa* and *Pparg* genes. Degradation of SETD5, which is mediated by APC/C E3 ubiquitin ligase, facilitates HAT recruitment to primed enhancers for hyperacetylation. Thus, the spatiotemporal dynamics for SETD5 residence in NCoR-HDAC3 co-repressor complex modulates enhancer transition from the primed to active state that is required for terminal differentiation of adipocytes.

Results

Primed enhancers of adipogenic master genes become active during the early phase of adipogenesis

To understand the regulation of chromatin modifications associated with enhancer activity during adipogenesis, we analyzed repressive H3K27me3, permissive H3K4me1, and active H3K27ac by chromatin immunoprecipitation sequencing (ChIP-seq) during

differentiation of cultured 3T3-L1 preadipocytes. Consistent with prior studies, C/EBPβ and C/EBPδ that are early pro-adipogenic transcription factors [16, 31], were expressed in preadipocytes but their transcript levels were further induced during the first 48 hrs of differentiation (Supplementary Fig. 1a). Mandrup and her colleagues, using the Hi-C technique, previously identified functional enhancers for *Cebpb* are located at +77 kb and +88 kb [32]. As shown in Supplementary Fig. 1b, we also observed that these enhancers displayed active enhancer signatures marked by the presence of both H3K4me1 (track 3) and H3K27ac (track 4) coupled with a paucity of H3K27me3 (track 2) in the same distal regions of *Cebpb* (e.g. +77 kb and +88 kb) and *Cebpd* (e.g. +62 kb and +98 kb) in preadipocytes before differentiation (i.e. 0h) indicating that these enhancers are already active before differentiation. By contrast, C/EBPα and PPARγ, both of which are late-adipogenic transcription factors [16], were expressed at very low levels early but are robustly induced between 24 and 48 hrs. of differentiation (Supplementary Fig. 1a). Supplementary Fig. 1c shows that before differentiation (0 h), genomic regions distal to *Cebpa* (e.g. +8 kb, +19 kb, and +53 kb) and *Pparg* (e.g. +60 kb and +158 kb) had H3K4me1 (track 3) but lacked H3K27me3 (track 2) and H3K27ac (track 5), indicating that these enhancers were in a "primed" state [33]. At 48 hrs of differentiation, these H3K4me1 enriched regions received additional H3K27ac modifications (Supplementary

Fig. 1c, tracks 4 and 6) indicating that these primed enhancers were converted into active enhancers. Time course ChIP-qPCR analysis confirmed that H3K27ac levels on *Cebpa* and *Pparg* enhancers were maintained very low during the early phase (~24 hrs) and were elevated at 48 hrs of differentiation (Supplementary Fig. 1d). Fig. 1a illustrates the transition from primed to active state during this period and the underlying mechanism has remained elusive.

Identification of SETD5 as a novel negative regulator of adipogenesis

To search for epigenetic enzymes that may keep enhancers in a primed state, we evaluated our prior transcriptome data for gene expression changes that occur during differentiation of 3T3-L1 adipocytes [21]. We found that mRNA expression of the putative histone modification enzyme SETD5 was down-regulated by two fold by 48 hrs of differentiation in response to a strong MDI adipogenic cocktail which contains methylisobutyl-xanthine, dexamethasone, and insulin and this down regulation was prevented by Wnt3a, a potent inhibitor of adipogenesis [14, 34] (Fig. 1b and Supplementary Fig. 1e). To investigate roles of SETD5 in adipogenesis, a V5-tagged SETD5 (SETD5-V5) retroviral expression construct (Fig. 1c) or an empty vector control were expressed using a weak LTR promoter [35] in 3T3-L1 preadipocytes. After stable transformation, we obtained two lines of SETD5-

transduced 3T3-L1 preadipocytes that express 5.6-fold and 15-fold higher expression of *Setd5* mRNA compared to those in empty vector transduced preadipocytes (Supplementary Fig. 1f). Empty vector or SETD5-transduced 3T3-L1 preadipocytes were treated with the MDI mixture and subjected to Oil Red O (ORO) staining after 8 days of differentiation. This revealed that both high (15-fold) and moderate (5.6-fold) ectopic over-expression of SETD5 showed inhibitory effects on lipid accumulation (Supplementary Fig. 1g) accompanied with a blunting in the induction of *Cebpa* and *Pparg* (Supplementary Fig. 1h). Because the mRNA expression of endogenous *Setd5* is reduced during the early phase of differentiation (Fig. 1b), we reasoned that sustained expression of SETD5 inhibited adipogenesis. In the following experiments, we used the cell line expressing the moderate level of (5.6-fold) of SETD5-V5 unless otherwise stated. Immunoblot analysis and ORO staining show that the inhibitory effect of SETD5 on adipogenesis was not overcome even by addition of the potent PPARγ synthetic full agonist troglitazone (Tro) (Fig. 1d, e). Transcriptome analysis showed that induction of *Cebpb* and *Cebpd* genes, whose transcripts are induced at the very early phase of differentiation, were not affected by sustained SETD5 expression (Fig. 1f). By contrast, SETD5 prevented the late induction (48 hrs) of *Cebpa* and *Pparg*, as well as expression of PPARγ target genes such as *Cd36* (Fig.1f).

To complement the sufficiency results, we evaluated SETD5 necessity by predicting that a decrease in SETD5 expression would enhance differentiation of 3T3-L1 preadipocytes (Fig. 1g). Because the MDI cocktail is very efficient in converting 3T3-L1 preadipocytes into mature adipocytes, we reasoned that it would be difficult to assess an increase in adipogenesis using MDI. Therefore, we used only DEX alone, which is much less efficient at inducing differentiation than the complete cocktail [14, 21, 36, 37]. Knockdown of SETD5 by two independent siRNAs resulted in increased expression of both *Cebpa* and *Pparg* over Dex alone and this was associated with a marked increase in lipid accumulation relative to the control siRNA transfected preadipocytes (Fig. 1h, i). Surprisingly, the effects of SETD5 knockdown were also observed even when strong complete MDI cocktail was used (Supplementary Fig. 1i).

SETD5 associates with NCoR-HDAC3 co-repressor complex and represses adipogenic genes

The conserved SET domain binds the methyl-donating cofactor S-adenosyl methionine which is required for their histone methyltransferase activity. To determine whether the SET domain is required for SETD5-mediated inhibition of adipogenesis, we constructed a V5-tagged SET domain deletion mutant (ΔSET) SETD5 and analyzed its function in

retrovirally transduced 3T3-L1 preadipocytes. Expression levels of WT and ΔSET mutant SETD5 proteins were very similar as confirmed by immunoblot analysis (Supplementary Fig. 1j). However, unexpectedly, ΔSET mutant blocked differentiation in response to the strong MDI cocktail very similarly to WT-SETD5 (Fig. 1j) and once again, this was not affected by inclusion of troglitazone (Tro) (Supplementary Fig. 1k). This result suggests that SETD5 inhibits adipocyte differentiation and lipid accumulation independently of its SET domain. However, we found that deletion of amino acids 437-918 (Δ437-918) blunted the inhibitory effect of SETD5 (Fig. 1j, Supplementary Fig. 1k), indicating that this region is required for SETD5-mediated inhibition of lipid accumulation during adipocyte differentiation.

To begin to study the mechanism of adipocyte differentiation repression through this region of SETD5, we performed a comprehensive proteomics analysis to find possible proteins that may interact with SETD5 through this region. Extracts from preadipocytes expressing V5-tagged SETD5 wild-type (WT) or the two deletion mutants (ΔSET or Δ437-918) were immunoprecipitated with anti-V5 antibody and the profiles of interacting proteins were compared after mass spectrometry. There were several peptide sequences that were immunoprecipitated in both WT and ΔSET SETD5 transduced preadipocytes but were absent in Δ437-918 transduced cells. These included peptides

corresponding to NCoR (also known as NCoR1), SMRT (also known as NCoR2), TBL1 (also known as TBL1X), TBLR1, SKI, and HDAC3 (Fig. 1k, blue solid circle) which is known to interact with SETD5 [27, 30, 38] suggesting that SETD5 associates with this co-repressor complex independent of its SET domain but dependent on the domain that was required for inhibition of adipogenesis. This is consistent with previous data showing a larger C-terminal deletion of SETD5 disrupts its interaction with HDAC3 [27, 30, 38]. Components of polymerase-associated factor (PAF1) complex (CTR9, CDC73, PAF1, and LEO1) [39], which is known to interact with SETD5 [27, 38], were also found in SETD5 co-immunoprecipitates, although these were present in all three samples (Fig. 1k, solid black circles). The putative interaction between SETD5 with several other proteins (e.g. PRR4B, PLRG1) was SET domain dependent (Fig. 1k, solid orange circles). Additionally, we observed the putative interaction with a multimeric ubiquitin E3 ligase APC/C complex, containing ANAPC1 and ANAPC2, and a ubiquitin E3 ligase RNF213 (Fig. 1k, solid pink circles, see also Fig. 3f).

Because the interaction with the NCoR and SMRT co-repressor complexes required the SETD5 domain that was essential to inhibit lipid accumulation, we explored this further. First, we depleted NCoR2 by siRNA in SETD5-transduced preadipocytes and showed that MDI dependent suppression of ORO accumulation by SETD5 was reversed

by NCoR2 depletion (Fig. 1l, m). Two other siRNAs targeted to *Ncor2* also restored lipid accumulation in SETD5-transduced cells (Supplementary Fig. 1l, m), indicating that NCoR2 is involved in SETD5 mediated inhibition of adipogenesis possibly through the formation of protein complex with SETD5. These results indicate that SETD5 associates with NCoR and HDAC to inhibit *Cebpa* and *Pparg* expression and adipogenesis.

SETD5 keeps enhancers in a primed state and its depletion leads to conversion into a hyperacetylated active state

To interrogate mechanisms by which SETD5 might alter chromatin to inhibit *Cebpa* and *Pparg* expression, we performed ChIP-seq for H3K27ac before (0 hr) and after differentiation (48 hrs) in empty vector (control) and SETD5-transduced preadipocytes. We identified 11,033 H3K27ac peaks that are elevated at 48 hrs of differentiation in control preadipocytes (Fig. 2a). These H3K27ac peaks were first classified into two groups based on the absence or presence of H3K4me3 mark, which represents active enhancers and promoters, respectively [5]. Among 9,546 active enhancers (i.e. H3K27 acetylated sites that lack H3K4me3 marks) at 48 hrs, forced expression of SETD5 repressed H3K27ac at 2,958 enhancers (31%) (Fig. 2a, class i) that includes enhancers of *Cebpa* and *Pparg* indicating that SETD5 inhibited H3K27 acetylation of enhancers during

48 hrs of early differentiation. SETD5, by contrast, increased H3K27 acetylation on certain enhancers (9%) (class iii). Among 1,487 promoters (i.e. presence of both H3K27ac and H3K4me3), SETD5 repressed H3K27ac at 396 promoters (27 %, class iv).

A gene ontology analysis showed that the enhancers whose H3K27ac levels were repressed by SETD5 (class i) were highly associated with lipid metabolic process, fat cell differentiation, and fatty acid metabolic process (Fig. 2b). Motif analysis showed that class i regions had motifs enriched in C/EBP and PPAR-RXR binding sequences (Fig. 2c), suggesting that SETD5-containig NCoR-HDAC3 repressor complex inhibits H3K27 hyperacetylation of enhancers (i.e. active state) bound by these transcription factors. Comparison of H3K27ac modification and genome wide binding sites of C/EBPβ and C/EBPδ (early adipogenic transcription factors) taken from the study of Mandrup and colleagues [19] showed that, among 2,958 H3K27ac sites that were found to be repressed in SETD5-transduced preadipocytes (i.e. sites kept in primed enhancers), 1,449 sites (49%) were bound by either C/EBPβ or C/EBPδ or both at 4 hrs of differentiation (Fig. 2d, left Venn diagram and right heatmap). Some of the SETD5-repressed H3K27ac sites were also binding sites for RXRα and PPARγ at 36 hrs of differentiation (Supplementary Fig. 2a, b). These results strongly suggest that SETD5 represses H3K27 acetylation to keep enhancers in a primed state during 24 hrs of differentiation through the binding sites

of C/EBPβ and C/EBPδ (see also motif analysis and co-immunoprecipitation shown later in Fig. 4e, f). Active enhancers of *Cebpa* (e.g. +8 kb, +35 kb, and +53 kb) and *Pparg* (e.g. +60 kb, +158 kb) in control preadipocytes were repressed in SETD5-V5 transduced preadipocytes at 48 hrs (Fig. 2e, compare tracks 2 and 4, and Fig. 2f). Transcription factors C/EBPβ and C/EBPδ were recruited to some of the above enhancers (e.g. *Cebpa* +8 kb and *Pparg* +60 kb) in control cells as early as at 4 hrs of differentiation [19] (Fig. 2e, tracks 5 and 6, highlighted in yellow). SETD5 was also recruited to these C/EBPβ and C/EBPδ binding sites (shown later in Fig. 4c, d). In a complementary experiment, siRNA mediated knockdown of SETD5 increased H3K27ac levels at enhancers of *Cebpa* (e.g. +8 kb and +53 kb) under DEX induction at 48 hrs induction (Fig. 2g). Together, these results indicate that SETD5 limits H3K27 acetylation at C/EBP binding site enhancers for *Cebpa* and *Pparg* genes.

Transient stabilization and APC/C-mediated proteasomal degradation of SETD5 during early adipogenesis

Because protein levels of SETD5 determine either a primed or active enhancer state, a key issue is how SETD5 protein levels are controlled during adipogenesis. We noticed that compared to before MDI induction, endogenous SETD5 protein levels were

transiently increased between 6-12 hrs and severely decreased at 48 hrs of differentiation (Fig. 3a). Curiously, we also noticed that a similar pattern for ectopically expressed V5-tagged SETD5, suggesting that SETD5 protein stability may be differentially regulated during this short window of differentiation (Fig. 3b, compare lanes 3-5 and lanes 6-9). Cell cycle analysis in Fig. 3c shows the first round of mitotic clonal expansion after MDI addition. G_0 arrested preadipocytes re-entered G_1 phase (0-12 hrs) followed by transition to S phase (12-21 hrs) and finally to G_2/M phase (21-36 hrs). The timing of the transient increase of SETD5 protein (6-12 hrs) corresponds to the G_1 phase while its decline corresponds to S and G_2/M phases (Fig. 3c, Supplementary Fig. 3a). Importantly, cell-cycling per se was not affected by ectopic SETD5 expression (Supplementary Fig. 3b).

We next asked whether this transient change in protein levels for SETD5 was due to changes in the rate of protein degradation because mRNA levels of endogenous SETD5 are reduced by approximately 50% at these time points (Fig. 1b). First, we measured SETD5 protein levels following MDI addition in the presence and absence of the proteasomal inhibitor MG132 which largely blocked the degradation of SETD5 protein (Fig. 3d, compare lanes 5-6 and 9-10) indicating that SETD5 is degraded via the ubiquitin-proteasome pathway. MG132 treatment increased a broad high molecular weight SETD5 signal recognized by anti-ubiquitin antibody, indicating that SETD5 is

ubiquitinated (Fig. 3e).

Next, we searched for a possible ubiquitin ligase responsible for cell-cycle dependent SETD5 degradation. From proteomic interaction data in Fig. 1k, two subunits of the anaphase-promoting complex/cyclosome (APC/C), ANAPC1 and ANAPC2 were found in immunoprecipitates of WT and the two mutant versions of SETD5 protein (i.e., wild-type, ΔSET, and Δ437-918) while ANAPC1 and ANAPC2 were not found in the immunoprecipitates from empty-virus transduced preadipocytes (Fig. 3f, Supplementary Fig. 3c). Among the APC/C subunits, the cullin subunit ANAPC2 and the RING domain subunit ANAPC11 compose the catalytic core and these two have critical roles in mediating the transfer of ubiquitin to substrates (Supplementary Fig. 3c) [22]. Another ubiquitin E3 ligase RNF213 was also found in immunoprecipitates of WT and two mutants of SETD5 protein (Fig. 3f).

mRNA levels of APC/C subunits themselves differed only slightly after MDI treatment and they were not altered by SETD5 over-expression (Supplementary Fig. 3d). However, The *Cdc20* coactivator of APC/C was very low during G_1 phase, and it was robustly increased during S and G_2/M phase (Fig. 3g). The time dependent induction of *Cdc20* concomitant with the decrease of SETD5 protein levels suggested that degradation of SETD5 might be triggered by CDC20 induction and consequent APC/C activation.

mRNA level of *Rnf213* was high before differentiation (0 hr) and was decreased by 12 hrs of differentiation (Supplementary Fig. 3e).

The stability of SETD5 protein was evaluated with a cycloheximide chase experiment where expression of the RING domain subunit ANAPC11 was knocked down and SETD5 levels were analyzed in the presence of cycloheximide (CHX), an inhibitor of translation. SETD5 was rapidly degraded in the presence of CHX in control siRNA transfected preadipocytes ($t_{1/2}$ = 2.0 hr), while SETD5 was markedly stabilized in ANAPC11 siRNA transfected preadipocytes ($t_{1/2}$ = 4.1 hr, Fig. 3h Supplementary Fig. 3f). Similarly, knockdown of APC/C coactivator CDC20 extended the half-life of SETD5 protein by a similar magnitude (Supplementary Fig. 3g, h). These results indicate that SETD5 is stabilized during G_1 phase where CDC20 level is low and APC/C is not active while during G_2/M phase of the first mitosis of early adipogenesis, SETD5 levels fall reciprocally with the induction of CDC20 and activation of APC/C.

SETD5 is transiently recruited to primed enhancers prior to enhancer activation

The data so far suggests that SETD5 is recruited to primed enhancers early in adipogenesis to prevent their premature activation. To evaluate this directly, we analyzed genome-wide localization of SETD5 during early adipogenesis. For this purpose, we

developed several monoclonal antibodies that recognize either the amino or carboxyl regions of SETD5 (Supplementary Fig. 4a, b). We chose one (IgG-F2104) that recognizes amino acids 43-93 and performed ChIP-seq for endogenous mouse SETD5 in preadipocytes at 6 hr after MDI treatment when SETD5 levels are still high and we identified 3,179 putative SETD5 binding sites (Supplementary Fig. 4c, d, e). This represents a very low number relative to most other ChIP-seq genome-wide analysis so we performed ChIP-seq in V5-tagged SETD5 (SETD5-V5) retrovirally transduced preadipocytes at 0 hr and at 6 hrs of induction. Consistent with the elevated SETD5-V5 protein levels, the number of genome wide binding sites was increased from 15,245 to 32,043 at 6 hrs of induction (Fig. 4a).

Similar to endogenous SETD5 (Supplementary Fig. 4a), most of the SETD5-V5 binding sites were located at intron and intergenic regions (Fig. 4a). When we compared the SETD5-V5 binding sites (6 hrs) with the H3K27ac data of 11,033 differentiation-dependent H3K27 acetylated regions at 48 hrs post MDI, 6,586 regions (60%) were occupied by SETD5-V5 at 6 hrs of differentiation (Fig. 4b, left). Importantly, at 6 hrs of differentiation, SETD5-V5 was recruited to H3K4me1 positive but H3K27ac negative regions (i.e. primed enhancers) and these regions were transformed to the dual marked H3K4me1 plus H3K27ac (i.e. active enhancers) at 48 hrs of differentiation where SETD5

protein was drastically reduced (Fig. 4b, right). A genome browser snapshot of the ChIP-seq data also showed that SETD5-V5 was recruited to *Cebpa* +8 kb and *Pparg* +60 kb enhancers at 6 hrs of differentiation (Fig. 4c, tracks 1 and 2), the sites where C/EBPβ and C/EBPδ were also bound [19] (Fig. 4c, tracks 9 and 10). Consistent with total SETD5-V5 protein levels (Fig. 3b), recruitment of SETD5-V5 to these enhancers peaked at 6 hrs were decreased to very low levels at 24 hrs of differentiation (Fig. 4d). Motif analysis showed that SETD5-V5 binding sites were enriched in Jun-AP1, C/EBP, and TEAD binding sequences (Fig. 4e). Because C/EBPβ and C/EBPδ are two transcription factors induced highly by 6 hrs of differentiation (Supplementary Fig. 1a), we hypothesized that SETD5 may associate with primed enhancers through these proteins. Immunoprecipitation and immunoblot analysis using cross-linked nuclear lysates showed an interaction between C/EBPβ and SETD5 at 6 hrs of differentiation (Fig. 4f) and this interaction was diminished at 24 hrs of differentiation as SETD5 was degraded by this time. In addition, recruitment of SETD5-V5 to primed enhancers of *Cebpa* and *Pparg* at 6 hr of differentiation were diminished via the knockdown of C/EBPβ and C/EBPδ (Fig. 4g and Supplementary Fig. 4f). These data indicate that SETD5 is recruited to enhancers via these transcription factors to prevent H3K27 hyperacetylation to keep the enhancers in their inactive but primed states.

SETD5 is co-recruited to primed enhancers with NCoR-HDAC3 complex and diminishes prior to enhancer activation

Our data so far suggest that SETD5 might function together with the NCoR-HDAC3 complex to inhibit adipogenesis. Because its SET domain is not required, SETD5 must function through a mechanism that is independent of its methylation activity. Comparison of our SETD5-V5 ChIP-seq data with previously reported NCoR and HDAC3 ChIP-seq data in 3T3-L1 preadipocyte [32] revealed that approximately 60% of NCoR (11,002 of 18,384) and 71% of HDAC3 (4,069 of 5,765) genomic binding sites are biding sites for SETD5-V5 at 6 hrs of differentiation (Fig. 5a, left Venn diagram). Recruitment of NCoR, HDAC3, and SETD5 were all increased after 4-6 hrs of differentiation relative to those of 0 hr (Fig. 5a, right heatmap). The ChIP-seq genome browser snapshot in Fig. 5b shows colocalization of SETD5-V5, NCoR, and HDAC3 to *Cebpa* and *Pparg* enhancers (e.g. *Cebpa* +8 kb and *Pparg* + 60 kb). These data support that SETD5-NCoR-HDAC3 transiently co-localize on these enhancers during the priming step and prior to enhancer activation. Our ChIP-qPCR confirmed that the increased recruitment of NCoR2 and HDAC3 to *Cebpa* and *Pparg* enhancers at 6 hrs of differentiation consistent with recent ChIP-seq data [32] (Fig. 5c, d). Although SETD5-V5 binding was undetectable at 24 hrs of

differentiation (Fig. 4d), NCoR2 and HDAC3 enhancer occupancy were still high at 24 hrs (Fig. 5c, d). Retrovirally expressed SETD5-V5 did not increase the recruitment of NCoR2 and HDAC3 to enhancers even at 6 hrs and 12 hrs of differentiation, where SETD5- V5 protein levels were the highest (Supplementary Fig. 5a, b). Biochemical analysis showed that SETD5 affected neither total nor HDAC3 specific histone deacetylase activities in vitro (Supplementary Fig. 5c, d). These data suggest that SETD5 may require NCoR-HDAC3 for its co-localization but SETD5 is likely not required for recruitment of NCoR-HDAC3 to enhancers.

To validate the contribution of APC/C mediated degradation of SETD5 to its recruitment to enhancers, ANAPC11 and CDC20 were depleted by siRNA mediated transfection. While SETD5 recruitment to enhancers at 24 hrs of differentiation was reduced compared with those at 6 hrs of differentiation (Fig. 4e, 5e, si-Ctr), knockdown of ANAPC11 or CDC20 kept SETD5 recruitment high at 24 hrs of differentiation (Fig. 5e) indicating that APC/C-mediated degradation of SETD5 contributes to its disappearance from primed enhancers prior to enhancer activation. These results indicate that SETD5-V5 increased co-localization with NCoR and HDAC3 at enhancers at 6-12 hrs of differentiation however, SETD5-V5 was lost through protein degradation by 24 hrs of differentiation (Fig. 5f).

SETD5-containg NCoR-HDAC3 complex restricts HAT recruitment to primed enhancers

Because these data suggested that SETD5 neither regulates NCoR-HDAC recruitment nor HDAC activity (Supplementary Fig. 5c, d) to decrease H3K27 acetylation on enhancer chromatin, we therefore hypothesized that SETD5 may limit recruitment of potential HATs to the enhancers. A comparison of ChIP-seq data for SETD5-V5 with the p300 HAT writer [32] showed that approximately 67% of p300 genomic binding regions (5,103 of 7,594 sites) were also binding sites for SETD5-V5 (Fig. 6a). A ChIP-seq genome browser snapshot shows both SETD5 and p300 HAT were recruited to primed enhancers (i.e. *Cebpa* +8 kb and *Pparg* +60 kb and +158 kb) immediately after differentiation (4–6 hrs) (Fig. 6b). Unfortunately, the anti-p300 antibody used in the previous study [32] is currently unavailable, so we examined HAT recruitment of CBP which is highly related to p300 [12]. A time course ChIP-qPCR analysis showed that while CBP recruitment to the primed enhancers for *Cebpa* was elevated by 6 hrs. after differentiation in control preadipocytes (Empty) (Fig. 6c), however, H3K27ac levels were kept low until 48 hrs. of differentiation (Fig. 6d). Interestingly, SETD5-V5 expression limited both recruitment of CBP throughout differentiation and prevented the increase in

H3K27ac at 48 hrs. This suggested that SETD5-V5 may restrict CBP recruitment to primed enhancers (Fig. 6c) and prevented the increase in H3K27ac (Fig. 6d). Note that NCoR-HDAC3 co-repressor were also recruited as early as 6 hrs. of differentiation but began to decrease after 24 hrs (Fig. 5c, d, f), while CBP recruitment remained elevated (Fig. 6c, Empty). When the complete induction MDI was used, depletion of SETD5 had minimal effects (data not shown). However, depletion of endogenous SETD5 by siRNA lead to a significant increase in the recruitment of CBP to *Cebpa* and *Pparg* enhancers when DEX alone was used to initiate adipocyte differentiation (Fig. 6e). These results indicate that SETD5-NCoR-HDAC3 complex restricts accessibility of HAT to primed enhancers, thereby regulating the time course of enhancer activation. When SETD5 protein diminishes via proteasomal degradation and consequently its recruitment to primed enhancers declines, HAT recruitment to primed enhancers increases to robustly drive master regulator gene expression and the adipogenic differentiation program (Fig. 6f).

Discussion

Strict temporal control of cell type-specific gene expression is essential for the exquisite timing and robust changes required for development and differentiation transitions and is

mediated through the combinatorial activation and repression at key enhancers. HAT co-activators and HDAC co-repressors collaborate to ensure correct enhancer acetylation and gene activation. The response of preadipocytes to external differentiation stimuli controls the pattern of recruitment of HAT co-activators along with antagonistic HDAC co-repressors to fine-tune the differentiation response. Mechanisms to actively control the addition and removal of key histone acetylations provides an appropriately sensitive system to ensure accurate and precise timing for gene expression transitions that drive differentiation down an irreversible course [12, 32]. In the current study, using protein interaction-based proteomics in the 3T3-L1 preadipocyte differentiation system, we identified SETD5 as a previously unappreciated component of the chromatin landscape that is required for adipocyte differentiation. Our studies show SETD5 interacts with the NCoR-HDAC3 complex to maintain enhancers for master genes of adipocyte differentiation in a histone hypoacetylated but "primed state" that is inactive. We show that the loss of SETD5 via proteasomal degradation synchronized with cell cycle triggers to influence enhancer hyperacetylation that is required for the transcriptional activation in lineage committed preadipocytes. SETD5 in an NCoR-HDAC3 complex restricts accessibility of HATs to enhancer chromatin but when SETD5 is lost from this complex via proteasomal degradation requiring the E3 ubiquitin ligase APC/C complex, associated

or recruited HATs then hyperacetylate enhancers leading to subsequent gene activation. Importantly, the transition mechanism is regulated by the APC/C co-activator CDC20 which is induced in parallel with SETD5 degradation.

In the original model of signal-dependent gene activation, key signals drive a unidirectional switch between NCoR-HDAC co-repressor and HAT co-activator in a simple two-step process [40, 41]. However, our study revealed that transition of adipogenic enhancers from a primed to active state is more dynamic and complex (Fig. 6f). Before differentiation (i.e. 0 hr), NCoR-HDAC3 co-repressor and HAT co-activator are both recruited weakly to primed enhancers that are bound by pioneer transcription factors (i.e. C/EBPβ and C/EBPδ) [42] but are functionally silent. (i) In early differentiation (until 6-12 hrs), both NCoR-HDAC3-SETD5 co-repressor complex and HAT co-activator are tethered to primed enhancers where SETD5 restricts accessibility of HATs to enhancer chromatin and keeps histones hypoacetylated and held in a primed state. (ii) As differentiation proceeds (i.e. after 24 hrs), as the first round of clonal expansion progresses, SETD5 is lost from the enhancer complex through active APC/C-mediated ubiquitination and degradation. (iii) In the absence of SETD5, the associated HAT leads to hyperacetylation and activation of enhancers and gene transcription (48 hrs). This mechanism allows precise temporal control of adipogenic master regulator genes (i.e.

Cebpa and *Pparg*) in synchronization with cell cycle regulation for cell fate decisions. Because SETD5 is ubiquitously expressed, this mechanism shown here in 3T3-L1 preadipocyte differentiation is likely to be applicable to other lineage committed cells. A SETD5-containg NCoR-HDAC3 complex may regulate enhancers recognized by other pioneer factors or cell type specific transcription factors in other lineage committed cells. This model can also explain why binding of pioneer factors do not facilitate transcription immediately until a critical time point of differentiation is reached, because colocalization of SETD5 with the NCoR-HDAC3 complex with C/EBPβ or C/EBPδ keep enhancers in a primed state.

Histone modification enzymes can function as a scaffold for co-activator or repressor recruitment via enzymatic activity-independent mechanisms [43, 44, 45, 46]. For example, the H3K9 demethylase JMJD1A acts as a cAMP-induced scaffold protein to stimulate enhancer-promoter chromatin looping of the *Adrb*1 gene in brown adipocytes through catecholamine mediated β-adrenergic receptor activation [45], and this bridging function is independent of the demethylase activity of JMJD1A. SETDB2 is predicted to be a H3K9 methyltransferase and it is induced during fasting in the liver through corticosteroid hormone mediated glucocorticoid receptor activation and in turn mediates enhancer-promoter interaction of *Insig2a* gene, whose gene product inhibits SREBP activation [46].

Like JMJD1A or SETDB2, we demonstrate that SETD5 works independent of its putative methyltransferase activity to keep enhancers in a primed state. This is by restricting the accessibility of HATs to enhancer chromatin via the formation of a protein complex with NCoR and HDAC3. In response to the adipocyte differentiation cue, absolute protein expression level of SETD5 is strictly controlled by degradation through the ubiquitination by E3 ubiquitin ligase APC/C. When SETD5 is lost from the complex due to its degradation, HAT recruitment is accelerated and their writing activity dominates HDAC erasing activity leading to hyperacetylation and activation of enhancers (Fig. 5f, 6f). This suggest that the spatiotemporal dynamics of SETD5-NCoR-HDAC3 complex determines enhancer transition from a primed to active state.

Our studies document a previously unrecognized role for the APC/C complex and specifically CDC20 in coordinating the regulated degradation of SETD5 and enhancer hyperacetylation that occurs between 24-48 hrs after MDI treatment. Because SETD5 depletion leads to enhancer activation (Fig. 2g), we focused on the mechanism for SETD5 degradation during S and G_2/M phase. SETD5 is also induced during 3-12 hrs. after MDI treatment which is at a time when the mRNA levels for SETD5 decrease by about half. We do not know the mechanism for the early induction of SETD5 expression. A ubiquitin ligase RNF213 was also found in the co-immunoprecipitates with SETD5 in our

proteomics analysis (Fig. 1k, 3f). In addition, *Rnf213* mRNA levels rapidly declined during the first 12 hrs of differentiation (Supplementary Fig. 3e), therefore, RNF213 mediated SETD5 protein degradation might account for the early induction of SETD5 expression. Interestingly, RNF213 is an E3 ligase with a dynelin-like core and a distinct ubiquitin transfer mechanism and plays an important role in lipid metabolism modulating lipotoxicity, fat storage, and lipid droplet formation [47, 48]. *RNF213* has been reported to be the major susceptibility factor for Moyamoya disease, a progressive cerebrovascular disorder that often leads to brain stroke in adults and children [49]. Whether RNF213 is responsible for the early induction of SETD5 protein levels remains to be determined.

While many of our conclusions for the genome wide studies rely on the SETD5-V5 data with the V5 antibody, we did observe the same trends with the IgG-F2104 antibody when analyzing endogenous SETD5. Thus, we are reasonably confident that the mechanism reflects the biological role for SETD5.

Several studies have noted that the cell cycle is linked to cell fate decisions via regulation of developmental transcription factors. For example, phosphorylation of Smad2/3 by cyclin and cyclin-dependent kinases renders embryonic stem cells susceptible to neuroectodermal differentiation [50]. Degradation of NeuroD2 by CDC20-APC/C regulates presynaptic differentiation [51]. We now showed that cell-cycle

synchronized induction of CDC20 activates APC/C-mediated degradation of SETD5 for adipogenic cell fate decision. Thus, this represents a novel mechanism where the induction of CDC20, a coactivator of the APC/C protein degradation complex, connects the cell-cycle machinery to a critical cell fate decision via transcriptional and epigenetic mechanisms.

Upon environmental stress, cells reversibly regulate enhancer status to alter gene expression and adapt to key environmental cues. Under long-term cold stimuli, enhancers of thermogenic genes in adipocytes become active (both H3K4me1 and H3K27ac positive), while warming reverses the enhancer status back to a primed state (e.g. only H3K4me1 positive) [52] that can be rapidly re-activated upon repeated cold exposure. During reprogramming to induced pluripotent stem cells, fibroblast-specific active enhancers are returned to a poised or inactive state [53]. Our studies reveal a previously unknown role for regulated protein degradation of SETD5 in modulating enhancer transition during adipocyte differentiation. It will be important to address whether the SETD5-NCoR-HDAC3 complex regulation revealed here performs a similar function in other developmental and differentiation pathways and programs.

Methods

A list of reagents and resource used is provided in Supplementary Table 1.

Antibodies

Mouse monoclonal IgG-F2104 and Z5721-234 against mouse SETD5 were developed by immunizing mouse with baculovirus particles displaying GP64 envelope fused to mouse SETD5 fragment (amino acids 49 to 93 or 1,241 to 1,291). IgG-F2104 which reacts with endogenous mSETD5 in immunoprecipitation and chromatin immunoprecipitation (ChIP) was used for ChIP-sequencing analysis.

Cell culture and Oil Red O staining

Mouse preadipocytes 3T3-L1 cell line was purchased from the American Type Culture Collection (Manassas, VA, USA). Cells were maintained in Dulbecco's modified Eagle's medium (DMEM) (Sigma-Aldrich, St. Louis, MO, USA) supplemented with 10% fetal bovine serum (FBS) (Thermo Fisher Scientific, Waltham, MA) and penicillin/streptomycin (Nacalai Tesque, Kyoto, Japan) (basal medium) at 37 °C in a 5% CO_2 atmosphere in a humidified incubator. For adipocytes differentiation, 2 days after reaching confluence (day 0), 3T3-L1 preadipocytes were treated with differentiation

medium containing insulin (1 μg/ml), 0.25 μM dexamethasone (DEX), and 0.5 mM isobutylmethylxanthine (MDI mixture) for 48 h followed by treatment with insulin (1 μg/ml) alone with medium replacement every 2 days as described previously [37] [36]. To inhibit adipogenesis, 3T3-L1 preadipocytes were exposed to 20 ng/ml Wnt3a (R&D Systems, Minneapolis, MN) in addition to MDI mixture for 48 h from the 1st day of induction. On day 8 of differentiation, the cells were stained with Oil Red O (ORO) as described previously [36, 37]. To analyze protein stability, 3T3-L1 preadipocytes were treated with MG132 (10 μM) or CHX (10 μg/ml).

Immunoblot analysis

Whole cell lysate (WCL) or nuclear fraction was prepared from cells at indicated day of differentiation [21] [36]. Aliquots of WCL or nuclear fraction were subjected to immunoblot analysis as described. Immunoblots were visualized by chemiluminescence using Super Signal West Dura Extended Duration Substrate (Thermo Fisher Scientific), and luminescent images were analyzed by ImageQuant LAS 4000mini (GE Healthcare, Chicago, IL, USA). Equal loading of the proteins was confirmed by the detection of histone H3, TBP, or HDAC1.

RNA interference

The duplexes of each small interfering RNA (siRNA), targeting mouse *Setd5* mRNA (corresponding to nucleotide 2,061-2,085 and 3,859-3,883 from start codon; Thermo Fisher Scientific), *Ncor2* (MSS209220), *Cebpb* (corresponding to nucleotide 1,179-1,203 from start codon), *Cebpd* (MSS273628), *Anapc11* (MSS287826), or *Cdc20* (MSS235609) and control siRNA (Med GC Duplexes #2 12935-112) were transfected into cells using Lipofectamine RNAi MAX reagent (Thermo Fisher Scientific) as described [36, 37]. ON-TARGETplus siRNA targeting mouse *Ncor2* (J-045364-05, J-045364-06) was purchased from Dharmacon (Lafayette, CO, USA).

Plasmid construction and retroviral transduction

To construct retroviral expression vector for SETD5 containing V5-tag at COOH-terminus, mouse SETD5 coding sequence was cloned to pMXs-IRES-puro vector driven weak LTR promoter [35]. Deletion mutants were constructed by inverse PCR using KOD Plus neo DNA polymerase (Toyobo, Osaka, Japan). To construct transient expression plasmids for SETD5 containing the FLAG-tag at NH_2-terminus and HDAC3 containing V5-tag at COOH-terminus, mouse SETD5 coding sequence and mouse HDAC3 coding sequence were cloned to pCAG-IRES-Bsd and pcDNA3.1, respectively. All PCR-

generated constructs were verified by DNA sequencing. Retroviruses were produced in Plat-E cells [54]. 3T3-L1 preadipocytes were infected by retrovirus and selected with puromycin as described [36, 37].

Identification of SETD5-interacting proteins

Retrovirally transduced 3T3-L1 preadipocytes were grown in a 15-cm dish and harvested. The pellet of cells was washed once with PBS and frozen at -80°C until use. All subsequent operations were carried out on ice or at 4°C. Each cell pellet was thawed out and allowed to swell in hypotonic buffer B (10 mM HEPES (pH 7.9), 10 mM KCl, 1.5 mM $MgCl_2$, 1 mM EDTA, 1 mM EGTA, 1 mM dithiothreitol, and a mixture of protease inhibitors (cOmplete, Mini, EDTA-free; Merck, Darmstadt, Germany)) for 30 min, passed through a 25-gauge needle five times, and centrifuged at 20,000 g for 1 min. The pellet was resuspended in 0.2 ml of buffer C (10 mM HEPES (pH 7.9), 10 mM KCl, 1 mM $MgCl_2$, 0.5% (v/v) Nonidet P-40, and a mixture of protease inhibitors) and sonicated on ice 10 times using 10-s pulses using a Sonifier cell disruptor model 250 (Branson Ultrasonics, Danbury, CT, USA), and then the debris was removed by centrifugation. Supernatants were collected, and buffer was exchanged to 50 mM Tris-HCl (pH 8.0), 100 mM KCl, 0.1 mM EDTA, 5% glycerol, 0.1% Nonidet P-40 by Econo-Pac 10DG (Bio-

Rad, Hercules, CA, USA), ultrafiltrated by Amicon Ultra-4 MWCO 30K (Merck Millipore, Burlington, MA, USA), and used for immunoprecipitation. The samples were incubated with control IgG or anti-V5 epitope antibody cross-linked with Dynabeads protein G (Thermo Fisher Scientific) and rotated for 18 h at 4 °C. The beads were washed three times with buffer containing 20 mM HEPES (pH 7.9), 200 mM KCl, 2 mM EDTA, 0.1% Nonidet P-40, after which the protein complexes were eluted with buffer containing 62.5 mM Tris-HCl (pH 6.8), 2% SDS, and 25% glycerol for 5 min at 95 °C. Each eluate was precipitated with methanol and chloroform, washed with ice-cold acetone, and centrifuged at 2,000 × *g* for 10 min as described [55]. Each pellet was airdried and resuspended in 25 mM NH_4HCO_3 buffer containing 25% (v/v) CH_3CN at room temperature. The samples were reduced in 1.2mM tris(2-carboxyethyl)phosphine for 15 min at 50°C and alkylated in 3 mM iodoacetamide for 30 min at room temperature, respectively. The samples were digested overnight with 100 ng of trypsin (Promega, Madison, WI, USA) at 37°C. Aliquots of trypsinized samples were analyzed by liquid chromatography-tandem mass spectrometry (LC/MS/MS) as we described previously [56]. Protein quantification was done by processing the acquired LC-MS data with the software Progenesis LC-MS (version 2.6; Nonlinear Dynamics, Newcastle, UK). MS/MSspectra from features with charge +2, +3, and +4 were exported and searched against the Swiss-

Prot database using Mascot (version 2.3; Matrix Science).

Co-immunoprecipitation

3T3-L1 preadipocytes transduced with SETD5-V5 were cross-linked with 1.5 mM ethylene glycol bis(succinimidylsuccinate) (Thermo Fisher Scientific) for 30 min at followed by second cross-linking by addition of 1% formaldehyde for 10 min. After cross-linking, nuclear fraction was prepared and subjected to immunoprecipitation with Dynabeads Protein G (Thermo Fisher Scientific) conjugated with anti-C/EBPβ (sc-150X) or control rabbit IgG. Immunoprecipitates were eluted with SDS sample buffer, de-crosslinked at 37 °C for 3 h, and subjected to immunoblot analysis.

HDAC activity assay

For total HDAC activity, nuclear fraction prepared from 3T3-L1 preadipocytes transduced with control empty virus or SETD5-V5 was subjected to in vitro assay using HDAC fluorometric activity assay kit (Cayman Chemical, Ann Arbor, MI, USA). For HDAC3 activity, HEK293 cells were co-transfected with plasmids encoding FLAG-SETD5 and HDAC3-V5, and nuclear fraction was subjected to immunoprecipitation with anti-V5 antibody or control mouse IgG. Co-immunoprecipitates of HDAC3-V5 were

subjected to in vitro assay using HDAC fluorometric activity assay kit. Background signal of mouse IgG control was subtracted from fluorescent signal of HDAC3-V5 co-immunoprecipitate to obtain HDAC3 activity.

Chromatin immunoprecipitation

The chromatin immunoprecipitation (ChIP) assays were performed as described previously [37] [45] [36]. For ChIP using anti-H3K27ac and anti-H3K4me1 antibodies, cells were cross-linked with 0.5% formaldehyde, while for ChIP using anti-H3K9me3 and anti-CBP antibodies, cells were cross-linked with 1% formaldehyde for 10 min. For ChIP using anti-V5-tag, anti-SETD5, anti-NCoR2, and anti-HDAC3 antibodies, cells were cross-linked with 1.5 mM ethylene glycol bis(succinimidylsuccinate) (Thermo Fisher Scientific) for 30 min at followed by second cross-linking by addition of 1% formaldehyde for 10 min. After cross-linking, nuclear fraction was prepared and sheared to 200-300 bp (for anti-H3K27ac and anti-H3K4me3) and ~2 kb (for other antibodies) by using SONIFIER 250 (Branson). Sonicated nuclear fraction was incubated overnight with each antibody pre-bound to Dynabeads Protein G (Thermo Fisher Scientific). ChIP DNA was purified using QiAquick PCR purification kit (Qiagen), and the concentration was measured by Qubit double-stranded DNA high sensitivity assay kit (Thermo Fisher

Scientific).

qPCR, ChIP-qPCR, and ChIP-seq analyses

qPCR was carried out in 384-well plates using ABI PRISM 7900HT sequence detection system (Applied Biosystems). All reactions were done in triplicate. mRNA expression was presented as fold change relative to indicated control after normalization to cyclophilin [45]. ChIP signals were presented as input percent as described [36]. All primer sequences used in this article are listed in Tables S2 and S3. ChIP-seq library was prepared using TruSeq ChIP library preparation kit (Illumina) or KAPA Hyper Prep Kit (Kapa Biosystems) according to the manufacturer's instructions. For ChIP-seq using anti-V5-tag and anti-SETD5 antibodies, ChIP DNA was sheared to ~200 bp by Covaris Acoustic Solubilizer (Covaris) before library preparation. ChIP-seq was done with Genome Analyzer IIx or HiSeq 2500 (Illumina) as previously described [45] [36].

Computational data analysis

For ChIP-seq data processing, all bound DNA fragments were mapped to UCSC build mm9 (NCBI Build37) assembly of the mouse genome by the mapping program ELAND based on the 5'-side 36-bp sequences. ChIP-seq signals were plotted in reads per million

mapped reads (RPM) and displayed on UCSC genome browser. To identify ChIP-seq enriched regions of RXRα and PPARγ, MACS program, a method appropriate for sharp peaks, was used under default setting [57 58]. For H3K27ac, SETD5-V5 and SETD5, SICER program, a method appropriate for broad peaks [59 60], was used under the following parameters: window size 200 bp; gap size 400 bp (H3K27ac) and 600 bp (SETD5-V5 and SETD5); *E*-value threshold, 100. Previously reported ChIP-seq data for H3K27ac, C/EBPβ, C/EBPδ, HDAC3, NCoR, and p300 [19 32] were used to analyze genomic binding regions by using MACS2 program [57 58]. Each enriched region was annotated to proximal genes within 50 kb. For a gene ontology analysis, DAVID 6.7 bioinformatics resources were used [61], and the p value is corrected for multiple hypothesis testing using the Benjamini-Hochberg method. Motif analysis was perfomed by using HOMER program [3].

Quantification and statistical analysis

Data are shown as mean ± SEM for independent experiments or mean ± SD for technical replicates. Statistical test was performed for two sets of data (Student's t-test) or comparisons of group (Tukey's post hoc comparison). P values denoted as *p < 0.05; **p < 0.01 (N.S., not significant).

Data and code availability

Gene expression microarray data and ChIP-seq data for H3K4me1, H3K27ac, SETD5-V5, and SETD5 were deposited in the Gene Expression Omnibus (GEO) database with accession numbers GSExxxxx. Other ChIP-seq data were already published and deposited in the GEO database (GSE73434) or the DNA data bank of Japan (DRA000378) [36 62].

References

1. Plank JL, Dean A. Enhancer function: mechanistic and genome-wide insights come together. *Molecular cell* **55**, 5-14 (2014).

2. Spitz F, Furlong EEM. Transcription factors: from enhancer binding to developmental control. *Nature Reviews Genetics* **13**, 613-626 (2012).

3. Heinz S*, et al.* Simple combinations of lineage-determining transcription factors prime cis-regulatory elements required for macrophage and B cell identities. *Mol Cell* **38**, 576-589 (2010).

4. Heinz S, Romanoski CE, Benner C, Glass CK. The selection and function of cell type-specific enhancers. *Nature reviews Molecular cell biology* **16**, 144-154 (2015).

5. Heintzman ND*, et al.* Distinct and predictive chromatin signatures of transcriptional promoters and enhancers in the human genome. *Nat Genet* **39**, 311-318 (2007).

6. Calo E, Wysocka J. Modification of enhancer chromatin: what, how, and why? *Mol Cell* **49**, 825-837 (2013).

7. Visel A*, et al.* ChIP-seq accurately predicts tissue-specific activity of enhancers. *Nature* **457**, 854-858 (2009).

8. Perissi V, Jepsen K, Glass CK, Rosenfeld MG. Deconstructing repression: evolving models of co-repressor action. *Nature Reviews Genetics* **11**, 109-123 (2010).

9. Guenther MG, Barak O, Lazar MA. The SMRT and N-CoR corepressors are activating cofactors for histone deacetylase 3. *Molecular and cellular biology* **21**, 6091-6101 (2001).

10. Codina A, Love JD, Li Y, Lazar MA, Neuhaus D, Schwabe JW. Structural insights into the interaction and activation of histone deacetylase 3 by nuclear receptor

corepressors. *Proc Natl Acad Sci U S A* **102**, 6009-6014 (2005).

11. Yang X-J, Seto E. The Rpd3/Hda1 family of lysine deacetylases: from bacteria and yeast to mice and men. *Nature reviews Molecular cell biology* **9**, 206-218 (2008).

12. Wang Z*, et al.* Genome-wide mapping of HATs and HDACs reveals distinct functions in active and inactive genes. *Cell* **138**, 1019-1031 (2009).

13. Rosen ED, MacDougald OA. Adipocyte differentiation from the inside out. *Nat Rev Mol Cell Biol* **7**, 885-896 (2006).

14. Okamura M*, et al.* COUP-TFII acts downstream of Wnt/beta-catenin signal to silence PPARgamma gene expression and repress adipogenesis. *Proc Natl Acad Sci U S A* **106**, 5819-5824 (2009).

15. Tang QQ, Otto TC, Lane MD. Mitotic clonal expansion: a synchronous process required for adipogenesis. *Proc Natl Acad Sci U S A* **100**, 44-49 (2003).

16. Farmer SRCP. Transcriptional control of adipocyte formation. *Cell Metab* **4**, 263-273 (2006).

17. Cristancho AG, Lazar MA. Forming functional fat: a growing understanding of adipocyte differentiation. *Nat Rev Mol Cell Biol* **12**, 722-734 (2011).

18. Inagaki T, Sakai J, Kajimura S. Transcriptional and epigenetic control of brown and beige adipose cell fate and function. *Nat Rev Mol Cell Biol* **17**, 480-495 (2016).

19. Siersbæk R*, et al.* Extensive chromatin remodelling and establishment of transcription factor 'hotspots' during early adipogenesis. *EMBO J* **30**, 1459-1472 (2011).

20. Nielsen R*, et al.* Genome-wide profiling of PPARgamma:RXR and RNA polymerase II occupancy reveals temporal activation of distinct metabolic pathways and changes in RXR dimer composition during adipogenesis. *Genes Dev* **22**, 2953-2967 (2008).

21. Wakabayashi K*, et al.* The peroxisome proliferator-activated receptor gamma/retinoid X receptor alpha heterodimer targets the histone modification enzyme PR-Set7/Setd8 gene and regulates adipogenesis through a positive feedback loop. *Mol Cell Biol* **29**, 3544-3555 (2009).

22. Watson ER, Brown NG, Peters J-M, Stark H, Schulman BA. Posing the APC/C E3 ubiquitin ligase to orchestrate cell division. *Trends in cell biology* **29**, 117-134 (2019).

23. Kimata Y. APC/C Ubiquitin Ligase: Coupling Cellular Differentiation to G1/G0 Phase in Multicellular Systems. *Trends Cell Biol* **29**, 591-603 (2019).

24. Grozeva D*, et al.* De novo loss-of-function mutations in SETD5, encoding a methyltransferase in a 3p25 microdeletion syndrome critical region, cause intellectual disability. *The American Journal of Human Genetics* **94**, 618-624 (2014).

25. Kuechler A*, et al.* Loss-of-function variants of SETD5 cause intellectual disability and the core phenotype of microdeletion 3p25. 3 syndrome. *European Journal of Human Genetics* **23**, 753-760 (2015).

26. Szczałba K*, et al.* SETD5 loss-of-function mutation as a likely cause of a familial syndromic intellectual disability with variable phenotypic expression. *American Journal of Medical Genetics Part A* **170**, 2322-2327 (2016).

27. Deliu E*, et al.* Haploinsufficiency of the intellectual disability gene SETD5 disturbs developmental gene expression and cognition. *Nat Neurosci* **21**, 1717-1727 (2018).

28. Moore SM*, et al.* Setd5 haploinsufficiency alters neuronal network connectivity and leads to autistic-like behaviors in mice. *Transl Psychiatry* **9**, 24 (2019).

29. Sessa A*, et al.* SETD5 Regulates Chromatin Methylation State and Preserves Global Transcriptional Fidelity during Brain Development and Neuronal Wiring. *Neuron* **104**, 271-289.e213 (2019).

30. Wang Z*, et al.* SETD5-Coordinated Chromatin Reprogramming Regulates Adaptive Resistance to Targeted Pancreatic Cancer Therapy. *Cancer Cell* **37**, 834-849.e813 (2020).

31. Cao Z, Umek RM, McKnight SL. Regulated expression of three C/EBP isoforms during adipose conversion of 3T3-L1 cells. *Genes & development* **5**, 1538-1552 (1991).

32. Siersbaek R*, et al.* Dynamic Rewiring of Promoter-Anchored Chromatin Loops during Adipocyte Differentiation. *Mol Cell* **66**, 420-435 e425 (2017).

33. Mikkelsen TS*, et al.* Comparative epigenomic analysis of murine and human adipogenesis. *Cell* **143**, 156-169 (2010).

34. Ross SE*, et al.* Inhibition of adipogenesis by Wnt signaling. *Science* **289**, 950-953 (2000).

35. Kitamura T*, et al.* Retrovirus-mediated gene transfer and expression cloning: powerful tools in functional genomics. *Experimental hematology* **31**, 1007-1014 (2003).

36. Matsumura Y*, et al.* H3K4/H3K9me3 bivalent chromatin domains targeted by lineage-specific DNA methylation pauses adipocyte differentiation. *Molecular cell* **60**, 584-596 (2015).

37. Inagaki T*, et al.* The FBXL10/KDM2B Scaffolding Protein Associates with Novel Polycomb Repressive Complex-1 to Regulate Adipogenesis. *J Biol Chem* **290**, 4163-4177 (2015).

38. Osipovich AB, Gangula R, Vianna PG, Magnuson MA. Setd5 is essential for mammalian development and the co-transcriptional regulation of histone acetylation. *Development* **143**, 4595-4607 (2016).

39. Van Oss SB, Cucinotta CE, Arndt KM. Emerging Insights into the Roles of the Paf1 Complex in Gene Regulation. *Trends Biochem Sci* **42**, 788-798 (2017).

40. Glass CK, Rosenfeld MG. The coregulator exchange in transcriptional functions of nuclear receptors. *Genes Dev* **14**, 121-141 (2000).

41. Raghav SK*, et al.* Integrative genomics identifies the corepressor SMRT as a gatekeeper of adipogenesis through the transcription factors C/EBPbeta and KAISO. *Mol Cell* **46**, 335-350 (2012).

42. Lee JE*, et al.* H3K4 mono- and di-methyltransferase MLL4 is required for enhancer activation during cell differentiation. *Elife* **2**, e01503 (2013).

43. Eskeland R*, et al.* Ring1B compacts chromatin structure and represses gene expression independent of histone ubiquitination. *Mol Cell* **38**, 452-464 (2010).

44. Sun Z*, et al.* Deacetylase-independent function of HDAC3 in transcription and metabolism requires nuclear receptor corepressor. *Mol Cell* **52**, 769-782 (2013).

45. Abe Y*, et al.* JMJD1A is a signal-sensing scaffold that regulates acute chromatin dynamics via SWI/SNF association for thermogenesis. *Nature Communications* **6**, 7052 (2015).

46. Roqueta-Rivera M*, et al.* SETDB2 Links Glucocorticoid to Lipid Metabolism through Insig2a Regulation. *Cell Metab* **24**, 474-484 (2016).

47. Ahel J*, et al.* Moyamoya disease factor RNF213 is a giant E3 ligase with a dynein-like core and a distinct ubiquitin-transfer mechanism. *eLife* **9**, (2020).

48. Sugihara M*, et al.* The AAA+ ATPase/ubiquitin ligase mysterin stabilizes cytoplasmic lipid droplets. *Journal of Cell Biology* **218**, 949-960 (2019).

49. Kamada F*, et al.* A genome-wide association study identifies RNF213 as the first Moyamoya disease gene. *Journal of Human Genetics* **56**, 34-40 (2011).

50. Pauklin S, Vallier L. The cell-cycle state of stem cells determines cell fate propensity. *Cell* **155**, 135-147 (2013).

51. Yang Y*, et al.* A Cdc20-APC ubiquitin signaling pathway regulates presynaptic differentiation. *Science* **326**, 575-578 (2009).

52. Roh HC*, et al.* Warming Induces Significant Reprogramming of Beige, but Not Brown, Adipocyte Cellular Identity. *Cell Metab* **27**, 1121-1137 e1125 (2018).

53. Papp B, Plath K. Epigenetics of reprogramming to induced pluripotency. *Cell* **152**, 1324-1343 (2013).

54. Morita S, Kojima T, Kitamura T. Plat-E: an efficient and stable system for transient packaging of retroviruses. *Gene therapy* **7**, 1063 (2000).

55. Wessel D, Flugge UI. A method for the quantitative recovery of protein in dilute solution in the presence of detergents and lipids. *Anal Biochem* **138**, 141-143 (1984).

56. Daigo K*, et al.* Proteomic analysis of native hepatocyte nuclear factor-4alpha (HNF4alpha) isoforms, phosphorylation status, and interactive cofactors. *J Biol Chem* **286**, 674-686 (2011).

57. Zhang Y*, et al.* Model-based analysis of ChIP-Seq (MACS). *Genome biology* **9**, R137 (2008).

58. Feng J, Liu T, Qin B, Zhang Y, Liu XS. Identifying ChIP-seq enrichment using MACS. *Nature protocols* **7**, 1728-1740 (2012).

59. Zang C, Schones DE, Zeng C, Cui K, Zhao K, Peng W. A clustering approach for identification of enriched domains from histone modification ChIP-Seq data. *Bioinformatics* **25**, 1952-1958 (2009).

60. Xu S, Grullon S, Ge K, Peng W. Spatial clustering for identification of ChIP-enriched regions (SICER) to map regions of histone methylation patterns in embryonic stem cells. *Methods Mol Biol* **1150**, 97-111 (2014).

61. Huang DW, Sherman BT, Lempicki RA. Systematic and integrative analysis of large gene lists using DAVID bioinformatics resources. *Nature protocols* **4**, 44-57

(2008).

62. Waki H*, et al.* Global mapping of cell type-specific open chromatin by FAIRE-seq reveals the regulatory role of the NFI family in adipocyte differentiation. *PLoS Genet* **7**, e1002311 (2011).

63. Kimura H, Hayashi-Takanaka Y, Goto Y, Takizawa N, Nozaki N. The organization of histone H3 modifications as revealed by a panel of specific monoclonal antibodies. *Cell structure and function* **33**, 61-73 (2008).

Acknowledgement

We thank Reiko Kuwahara and Akashi Taguchi-Izumi for technical assistance; Minori Yoshio for secretary assistance; Dr. Toshio Kitamura for pMXs-puro plasmid; and other members of the Sakai laboratory for helpful discussion. We thank Dr. Kai Ge for helpful discussion. This study was supported by grants-in-aid for scientific research (to Y.M. and J.S.), and for scientific research on innovative areas (to J.S.) from the Ministry of Education, Science, Sports and Culture (MEXT), AMED-CREST, under Grant Number JP20gm1310007 (to Y.M. S.T., and J.S.), Japan and grants from the Naito Foundation and Takeda Science Foundation.

Author Contributions

Y.M. and J.S. directed the study and wrote the paper. T.F.O. critically commented and edited the paper. Y.M., R.I., A.Y., R.Y., K.M., H.H., H.F., Y.A., A.U., and S.O. performed experiments. T.T. and T.Kawamura performed proteomics analysis. H.A. and Y.W. supported ChIP-seq, and Y.M., R.N., S.Y., and S.T. analyzed ChIP-seq data. H.K. provided materials. S.I., T.Kodama, T.I., and K.N. commented on the paper. All authors reviewed the results and approved the final version of the manuscript.

Competing interests

The authors declare no competing interests.

Additional information

Supplemental information is available for this paper at https://doi.org/xxxxx

Materials & Correspondence

Correspondence and requests for materials should be addressed to Y.M. or J.S.

Tables

Supplementary Table 1. List of reagent and resource.

REAGENT or RESOURCE	SOURCE	IDENTIFIER
Antibodies		
Anti-human PPARγ mouse mAb	[21]	IgG-A3409
Anti-human RXRα mouse mAb	[21]	IgG-K8508
Anti-H3K27ac mouse mAb	[63]	9E2H19
Anti-H3K9me3 mouse mAb	[63]	2F3
Anti-mouse SETD5 mouse mAb	This paper	IgG-F2104
Anti-mouse SETD5 mouse mAb	This paper	IgG-Z5721-234
Anti-TBP	Novus Biologicals	Cat#NB500-700
Anti-V5 mouse mAb	Thermo Scientific	Cat#R960-25
Anti-Histone H3	Abcam	Cat#ab1791
Anti-HDAC1	Santa Cruz	Cat#sc-8410
Anti-HDAC3	Abcam	Cat#ab7030
Anti-NCoR2	Abcam	Cat#ab5802
Anti-C/EBPβ rabbit pAb	Santa Cruz Biotechnology	Cat#sc-150x
Anti-C/EBPβ mouse mAb	Santa Cruz Biotechnology	Cat#sc-7962
Anti-CBP rabbit mAb	Cell Signaling Technology	Cat#7425
Anti-H3K4me1	Abcam	Cat#ab8895
Anti-Multi ubiquitin mAb	Medical and Biological Laboratories	FK2
Anti-mouse IgG-HRP	Sigma-Aldrich	Cat#A4416
Anti-rabbit IgG-HRP	Sigma-Aldrich	Cat#A0545
Bacterial plasmid and Virus Vector		
pMXs-IRES-Puro	Cosmo Bio	RTV-014
Chemicals, Peptides, and Recombinant Proteins		
DMEM High Glucose	Sigma-Aldrich	Cat#D6429
Fetal Bovine Serum	Thermo Fisher Scientific	Cat#10270

Penicillin-Streptomycin Mixed Solution	Nacalai Tesque	Cat#09367-34
3-Isobutyl-1-methylxanthine	Sigma-Aldrich	Cat#I5879
Dexamethasone	Sigma-Aldrich	Cat#D4902
Insulin	Sigma-Aldrich	Cat#I5523
Wnt3a	R&D Systems	Cat#5036-WN-010/CF
Puromycin	Sigma-Aldrich	Cat#P8833
Oil Red O	Nacalai Tesque	Cat#25633-92
Super Signal West Dura Extended Duration Substrate	Thermo Fisher Scientific	Cat#34075
Lipofectamine RNAiMAX Transfection Reagent	Thermo Fisher Scientific	Cat#13778150
Stealth RNAi siRNA Negative Control Med GC Duplex #2	Thermo Fisher Scientific	Cat#12935-112
KOD Plus Neo DNA polymerase	Toyobo	Cat#KOD-401
ISOGEN Reagent	Nippon Gene	Cat#315-02504
Formaldehyde Solution	FUJIFILM Wako	Cat#064-00406
Sequencing Grade Modified Trypsin	Promega	Cat#V5111
Ethylene glycol bis(succinimidylsuccinate)	Thermo Fisher Scientific	Cat#21565
Dynabeads Protein G for Immunoprecipitation	Thermo Fisher Scientific	Cat#10004D
Protein G Sepharose 4 Fast Flow	GE Healthcare	Cat#17061801
Critical Commercial Assays		
HDAC Fluorometric Activity Assay Kit	Cayman Chemical	Cat#10011563
QIAquick PCR Purification Kit	Qiagen	Cat#28106
Qubit Double-stranded DNA High Sensitivity	Thermo Fisher Scientific	Cat#32854

Assay Kit		
TruSeq ChIP Library Preparation Kit	Illumina	Cat#RS-122-2001 or RS-122-2002
KAPA Hyper Prep Kit	Kapa Biosystems	Cat#KK8502
Deposited Data		
RAW and analyzed ChIP-seq data	This paper	GEO: GSExxxxxx
Gene expression microarray data	This paper	GEO: GSExxxxxx
Experimental Model: Cell Line		
3T3-L1	ATCC	ATCC CL-173
Plat-E	Cosmo Bio	RV-101
Software and Algorithms		
MACS	[57]	http://liulab.dfci.harvard.edu/MACS/
MACS2	[57]	https://github.com/taoliu/MACS
SICER	[59]	https://home.gwu.edu/~wpeng/Software.htm
DAVID6.7	[61]	https://david-d.ncifcrf.gov/
HOMER	[3]	http://homer.ucsd.edu/homer/

Supplementary Table 2. List of RT-qPCR primers.

Gene	Forward primer	Reverse primer
Setd5	5'-CGTCGCCCGTAGAGGAACGC-3'	5'-CCCCTGCTCATTCCCCTGCACT-3'
Cebpa	5'-AGATGAGGGAGTCAGGCCGT-3'	5'-CGGAAAGTCTCTCGGTCTCAA-3'
Pparg	5'-CAAGAATACCAAAGTGCGATCAA-3'	5'-GAGCTGGGTCTTTTCAGAATAATAAG-3'
Ncor2	5'-CAAAAGGTCCCCAGAACCCAG-3'	5'-TTCCCCGTCTCGATACAGCAG-3'
Cebpb	5'-CAAGAAGACGGTGGACAAGCTGAG-3'	5'-GACAGCTGCTCCACCTTCTTCTG-3'
Cebpd	5'-TCGACTTCAGCGCCTACATTGAC-3'	5'-CCGCTTTGTGGTTGCTGTTGA-3'
Anapc2	5’-CCCAGGCTGACCAGAAGGAA-3’	5’-CCGGAGCATGCTGTAGATACG-3’
Anapc11	5’-GCTCTGGGTAGCCAATGATGAG-3’	5’-GCAGTCATCACCAGGCACCTT-3’
Cdc20	5’-GTCACGGCTTTGCCCAGAAC-3’	5’-GACCCGTGCTGTGTGTCCTT-3’

Supplementary Table 3. List of ChIP-qPCR primers.

Gene	Forward primer	Reverse primer
Cebpa -0.8 kb	5'-GTGGTGGTGTCCCGAACACT-3'	5'-CAGGCCAGAGCGATAGGATT-3'
Cebpa + 1 kb	5'-AACAGCAACGAGTACCGGGT-3'	5'-CGTCTCCACGTTGCGTTGT-3'
Cebpa + 8 kb	5'-CAGCTGGACTTAGTTGCCAAGC-3'	5'-TCTGACGGGTCCTAACCTGATG-3'
Cebpa +19 kb	5'- GCCCCACCAGGGATCTAGA-3'	5'- GGAAATGAGTCAGACAGCCATAAA-3'
Cebpa +35 kb	5'-CCCCAATCTTCCCTCAAATGA-3'	5'-GGAGCCCGGAACCAGAA-3'
Cebpa +53 kb	5'-TACCGCCGTTTCCCAAAC-3'	5'-TACCGCCGTTTCCCAAAC-3'
Pparg +60 kb	5'-GTTAGCAGTTTGGCACAGCTAGG-3'	5'-ATCAGGAAAACTCTGGCTTCTTG-3'
Pparg +158 kb	5'-TCCACAGAACAGGGCGATG-3'	5'-AAAGAAACCCAGCCCAGGC-3'
Hoxc13	5'-TGTCCTCCAGGGCTAAGGA-3'	5'-AGGTAGCCGGGCATTGC-3'
Ppib	5'-CTCACCCCAACTAGTCTAATCC-3'	5'-GTGACACACAGTGACTAACTTCC-3'

Figures

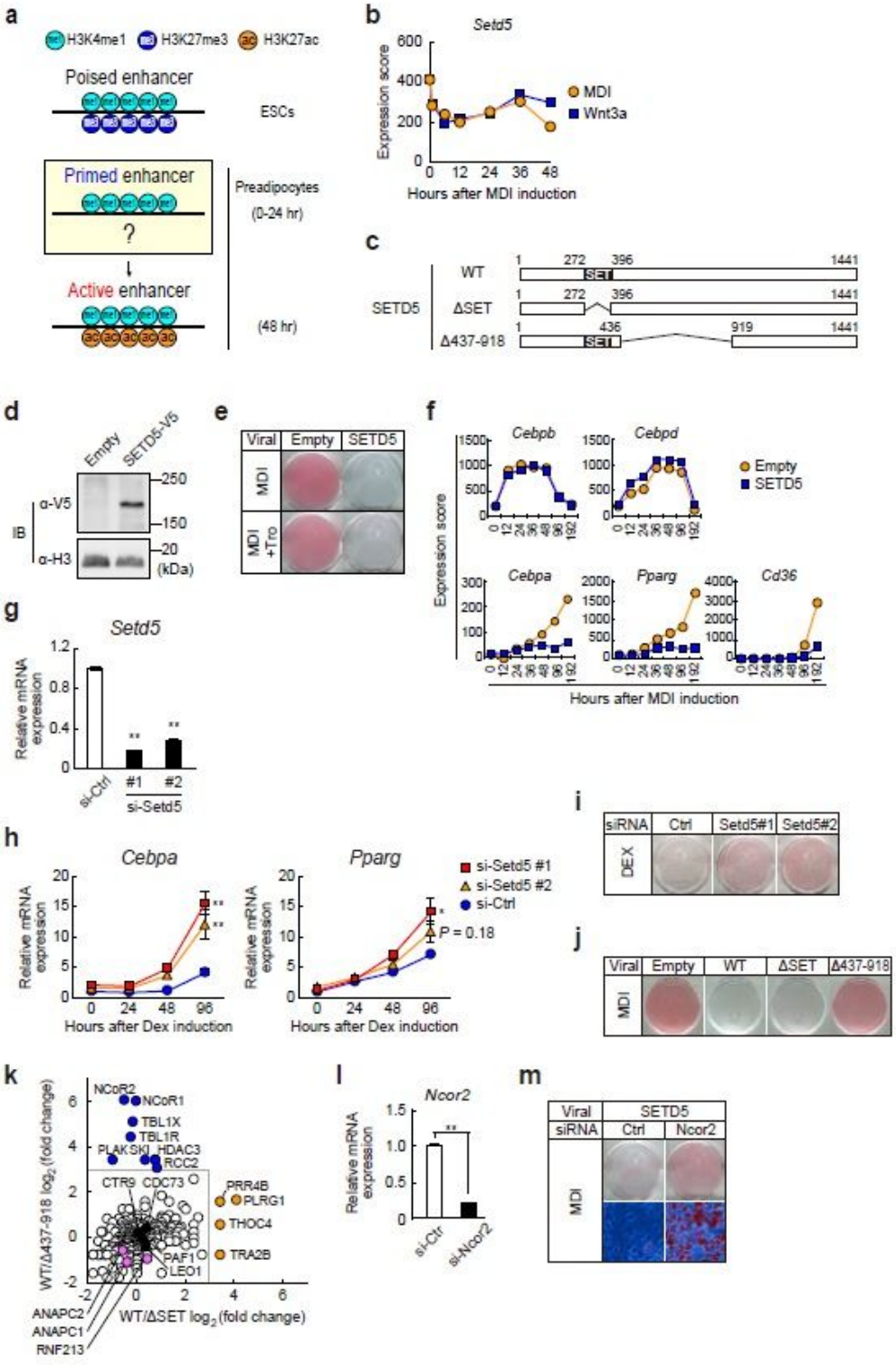

Figure 1

SETD5 associates with NCoR and HDAC to inhibit Cebpa and Pparg induction during adipogenesis. a Schematic illustration of enhancer states. Poised enhancer in embryonic stem cells (ESCs) is characterized by the presence of H3K4me1 and H3K27me3. Primed enhancer is characterized by the

presence of only H3K4me1, while active enhancer is characterized by the presence of both H3K4me1 and H3K27ac 6. b Setd5 gene expression during 3T3-L1 adipogenesis. Microarray data are from the previously published paper 21. c Schematic representation of mouse SETD5 protein and its mutants. SET domain is located at amino acids 273-395 of SETD5. d Retroviral expression of SETD5 in 3T3-L1 preadipocytes. Nuclear proteins from 3T3-L1 preadipocytes transduced with empty virus or SETD5-V5 were subjected to immunoblot (IB) analysis. Equal loading of the proteins was confirmed with by blotting with anti-histone H3 (H3) antibody. e ORO staining of 3T3-L1 preadipocytes transduced with empty virus or SETD5. Preadipocytes were induced with MDI mixture or MDI mixture plus troglitazone (Tro) and stained on day 8 of differentiation. f Transcriptional changes of adipogenic genes in SETD5-transduced 3T3-L1 preadipocytes during adipogenesis. Cells were harvested at the indicated times of differentiation, and transcriptional analyses were carried out using a microarray. g, h siRNA-mediated knockdown of SETD5 in 3T3-L1 preadipocytes. Setd5 (g), Cebpa, and Pparg (h) mRNA expression was quantified by qPCR. Cyclophilin mRNA was used as the invariant control. Data are represented as mean ± SEM of three independent experiments. Statistical test was performed for comparisons of group (Tukey's post hoc comparison). *p<0.05; **p<0.01. i ORO staining of SETD5 knocked-down 3T3-L1 preadipocytes. Preadipocytes were induced with Dex, and ORO staining was performed at day 8 of differentiation. j ORO staining of 3T3- L1 preadipocytes transduced with empty virus, SETD5, or mutants. Preadipocytes were induced with MDI mixture and stained on day 8 of differentiation. k Proteomics analysis of SETD5 interacting proteins. Nuclear proteins from WT-, ΔSET-, and Δ437-918-SETD5- transduced preadipocytes were subjected to immunoprecipitation with anti-V5 antibody followed by trypsin digestion and mass spectrometry. Color code: proteins lost (less than 2- 3-fold) by deletion of a.a. 437-918 (blue); proteins lost by deletion of SET domain (orange); proteins not affected by deletion of a.a. 437-918 or SET domain (white). Proteins of PAF1 complex are highlighted in black. Proteins of APC/C complexes and RNF213 are highlighted in pink. l siRNA-mediated knockdown of NCoR2 in SETD5-transduced 3T3-L1 preadipocytes. Ncor2 mRNA expression was quantified by qPCR. Cyclophilin mRNA was used as the invariant control. The experiments were performed three times, and the representative one is shown. Error bars represent mean ± SD of three technical replicates (**p < 0.01, Student's t test). m ORO staining of NCoR2 knocked-down, SETD5-transduced 3T3-L1 preadipocytes. Preadipocytes were induced with MDI mixture, and ORO staining was performed at day 8 of differentiation.

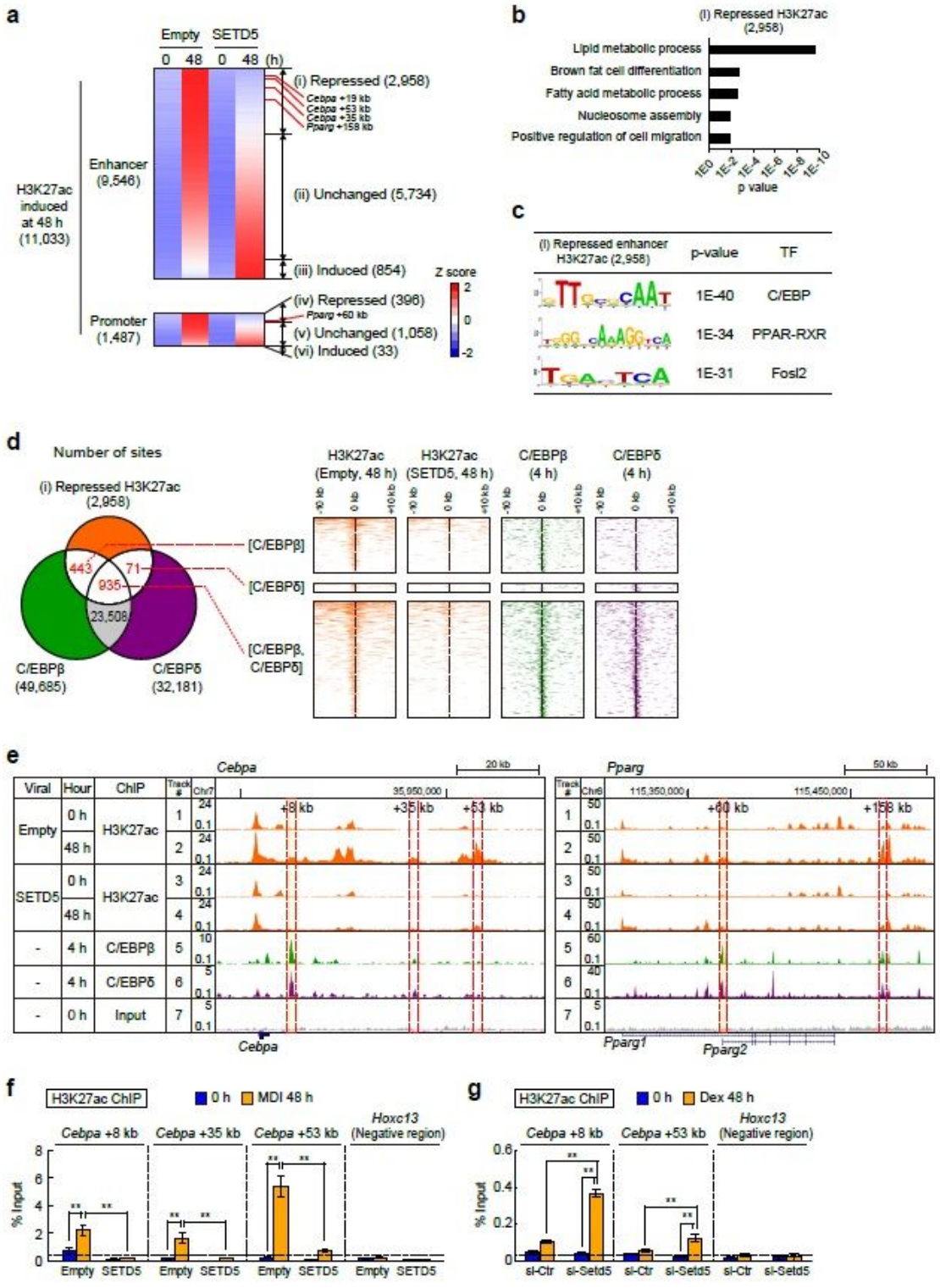

Figure 2

SETD5 inhibits H3K27 acetylation and enhancer activation of adipogenic genes. a Heatmap representation of H3K27 acetylation during 3T3-L1 adipogenesis. Color intensity represents Z-score of H3K27ac signals in 3T3-L1 preadipocytes transduced with empty virus or SETD5 at indicated day of differentiation. There were 11,033 H3K27ac enriched regions that were induced by differentiation stimuli (48 hrs) in control preadipocytes. These regions were classified into distal enhancer (9,546 regions) and

promoter (1,487 regions) based on the absence and presence of H3K4me3 signals. H3K27ac enriched regions were further classified into repressed (less than 0.5-fold), induced (more than 2-fold), and unchanged by SETD5 transduction. b Gene ontology (GO) analysis of differentiation-induced and SETD5-repressed H3K27ac enriched enhancer regions. GO analysis was performed by DAVID 6.7 bioinformatics resources. c Motif analysis of differentiation-induced and SETD5-repressed H3K27ac enriched enhancer regions. Motif analysis was performed by Homer bioinformatics resources 3. d Venn diagram and heatmap representation of differentiation-induced and H3K27ac enriched regions and C/EBPβ and C/EBPδ binding regions. Among differentiationinduced and SETD5-repressed H3K27ac enriched enhancer regions, 443 regions were bound by C/EBPβ, 71 regions were bound by C/EBPδ, and 935 regions were bound by both. Heatmap shows ChIP-seq data for H3K27ac, C/EBPβ, and C/EBPδ at a 20-kb region centered on H3K27ac enriched region. ChIP-seq for C/EBPβ and C/EBPδ was from the previously published paper 19. e Genome browser representation for H3K27ac, C/EBPβ, and C/EBPδ on adipogenic genes. 3T3-L1 preadipocytes transduced with empty virus or SETD5 were subjected to ChIP-seq for H3K27ac at indicated day of differentiation. Tracks 1, 2, and 7 are the same data as Supplementary Fig. 1c. ChIP-seq for C/EBPβ and C/EBPδ was from the previously published paper 19. f ChIP-qPCR analysis of H3K27ac on Cebpa gene during adipogenesis. 3T3-L1 preadipocytes transduced with empty virus or SETD5 were subjected to ChIP-qPCR analysis of H3K27ac at indicated time after MDI induction of differentiation. Data are represented as mean ± SEM of three to four independent experiments. g ChIPqPCR analysis of H3K27ac on Cebpa gene during adipogenesis. 3T3-L1 preadipocytes transfected with siRNA targeted to Setd5 were subjected to ChIP-qPCR analysis of H3K27ac at indicated time after Dex induction of differentiation. The experiments were performed twice, and the representative one is shown. Data are represented as mean ± SD of three technical replicates. Statistical test was performed for comparisons of group (Tukey’s post hoc comparison). **p<0.01.

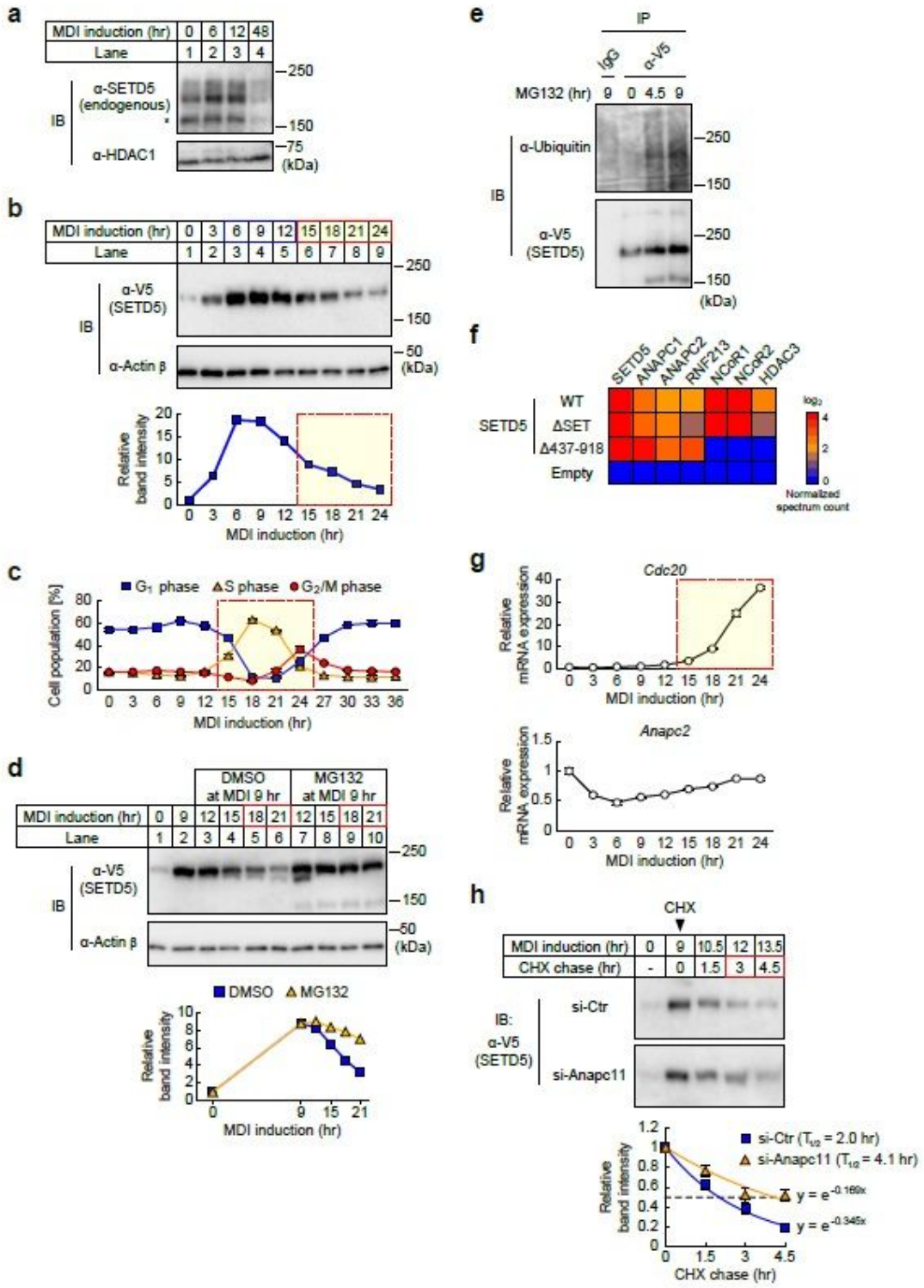

Figure 3

SETD5 is transiently stabilized and degraded by APC/C and proteasome during the early adipogenesis. a Immunoblot showing expression of endogenous SETD5 in 3T3- L1 preadipocytes during the early adipogenesis. Equal loading of the protein was confirmed by blotting with anti-HDAC1 antibody. b Immunoblot showing expression of SETD5-V5 in SETD5-transduced 3T3-L1 preadipocytes. Equal loading of the proteins was confirmed by blotting with anti-actin β antibody. Graph shows band intensity of

SETD5-V5 at indicated time after MDI induction. The experiments were performed three times, and the representative one is shown. c Cell cycle analysis of empty virus-transduced 3T3-L1 preadipocytes. The ratios of the cells at G1, S, or G2/M phase of preadipocytes during differentiation are shown. Error bars represent mean ± SD of three technical replicates. d Immunoblot showing expression of SETD5-V5 in SETD5-transduced 3T3-L1 preadipocytes treated with MDI and MG132. Equal loading of the proteins was confirmed by blotting with anti-actin β antibody. Graph shows band intensity of SETD5-V5 at indicated time after MDI induction. e Immunoblot showing ubiquitinated SETD5-V5. SETD5-transduced 3T3-L1 preadipocytes were treated with MDI and then MG132 at 9 hr after MDI induction. Preadipocytes were subjected to immunoprecipitation using anti-V5 antibody and immunoblotting with anti-ubiquitin and anti- V5 antibodies. f Heatmap representing abundance of APC/C subunits and RNF213 in SETD5-V5 immunoprecipitates. Nuclear proteins from WT-, ΔSET-, or Δ437-918-SETD5- transduced preadipocytes and control empty virus-transduced preadipocytes were subjected to immunoprecipitation with anti-V5 antibody followed by trypsin digestion and mass spectrometry. Spectrum count for each protein was normalized by spectrum count for common region of SETD5 (a.a. 1 to a.a. 272 and a.a. 919 to a.a. 1441). g Expression of mRNAs of APC/C subunits during the early adipogenesis. mRNA expression of Cdc20 and Anapc2 in SETD5-V5-transduced preadipocytes were quantified by qPCR. Cyclophilin mRNA was used as the invariant control. The experiments were performed twice, and the representative one is shown. Data are represented as ± SD of three technical replicates. h Immunoblot showing SETD5-V5 stability by the cycloheximide chase assay. 3T3-L1 preadipocytes transduced with SETD5-V5 were transfected with control siRNA or siRNA targeted to Anapc11 and induced for differentiation with MDI mixture. Preadipocytes were treated with cycloheximide (CHX) at 9 hrs after MDI induction and subjected to immunoblot analysis with anti-V5 at indicated time of differentiation. The experiments were performed three times, and the representative immunoblot is shown. The graph shows regression analysis of SETD5-V5 protein stability after CHX treatment. Data are represented as mean ± SEM of three independent experiments. Protein half-life (T1/2) was calculated based on exponential decay curve fit to the average data at each time point.

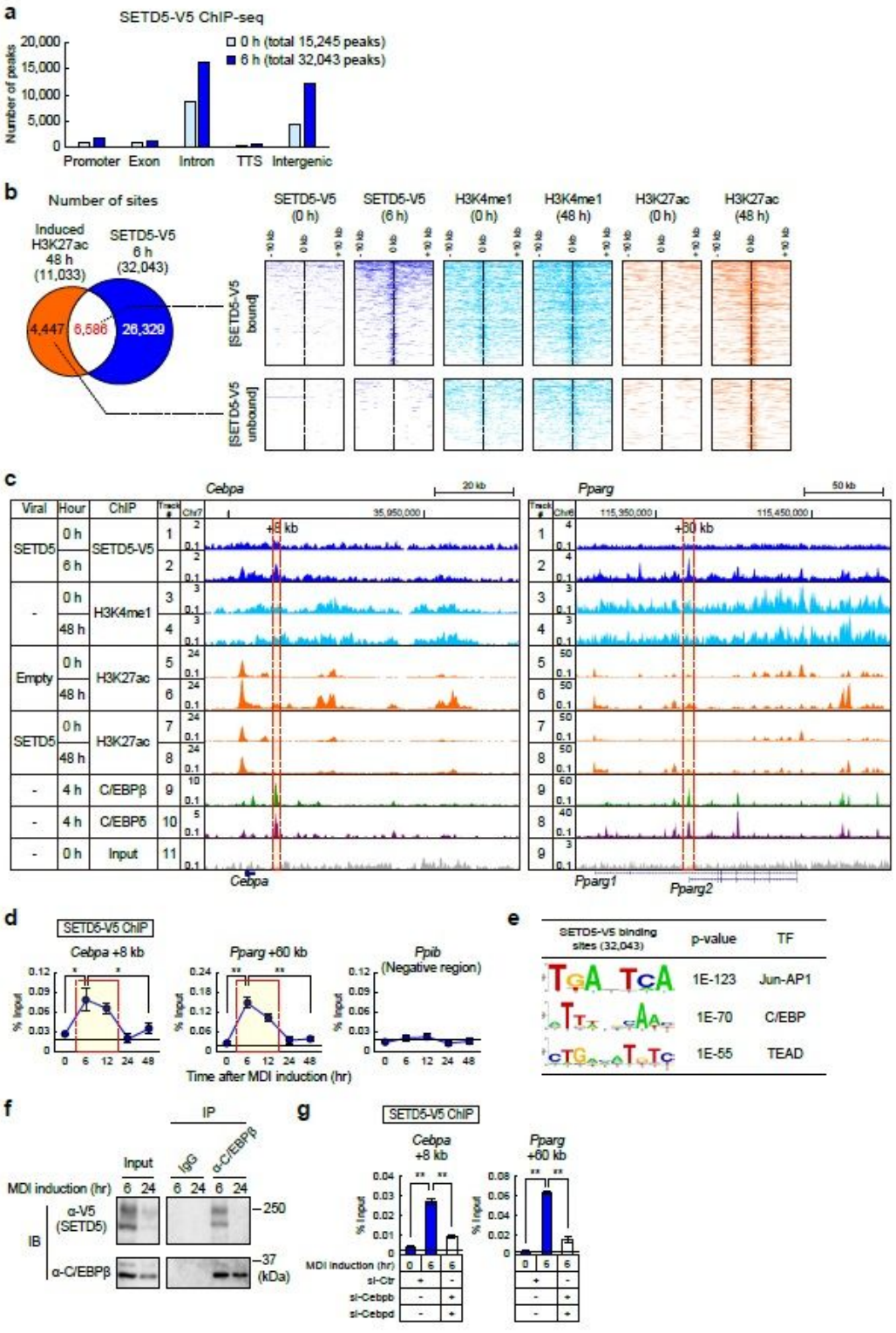

Figure 4

SETD5 is recruited to primed enhancers and diminishes prior to enhancer activation. a Genome-wide distribution of SETD5-V5 before (0 hr) and 6 hrs of differentiation in 3T3-L1 preadipocytes. TTS, transcription termination site. b Venn diagram (left) and heatmap (right) representations of genomic regions occupied by SETD5-V5, H3K4me1, and H3K27ac. Heatmap analysis showing ChIP-seq data for SETD5-V5, H3K4me1, and H3K27ac at a 20-kb region centered on SETD5-V5 binding regions. c Genome

browser representation for SETD5-V5, H3K4me1, H3K27ac, C/EBPβ, and C/EBPδ on Cebpa and Pparg genes in 3T3-L1 preadipocytes. Tracks 3-11 are the same data as Supplementary Fig. S1c or Fig. 2e. d ChIP-qPCR analysis of SETD5-V5 on Cebpa and Pparg genes during the early adipogenesis. 3T3-L1 preadipocytes transduced with SETD5-V5 were subjected to ChIP-qPCR analysis using anti-V5 antibody. Data are represented as mean ± SEM of three to four independent experiments. Statistical test was performed for comparisons of group (Tukey's post hoc comparison). *p<0.05; **p<0.01. e Motif analysis of SETD5-V5 binding sites at 6 hrs of differentiation. Motif analysis was performed by Homer bioinformatics resources 3. f Co-immunoprecipitation assay showing interaction of SETD5-V5 with C/EBPβ. 3T3-L1 preadipocytes transduced with SETD5-V5 at indicated time of differentiation were cross-linked with ethylene glycerol bis(succinimidyl succinate) and subjected to immunoprecipitation using anti-C/EBPβ antibody. Immunoprecipitates were decrosslinked and examined by immunoblotting using anti-V5 and anti-C/EBPβ antibodies. g ChIP-qPCR analysis of SETD5-V5 on Cebpa and Pparg genes under knockdown of C/EBPβ and C/EBPδ. 3T3-L1 preadipocytes transduced with SETD5-V5 were transfected with control siRNA or siRNA targeting to Cebpb and Cebpd and subjected to ChIP-qPCR analysis using anti-V5 antibody. Data are represented as mean ± SEM of three independent experiments. Statistical test was performed for comparisons of group (Tukey's post hoc comparison). *p<0.05; **p<0.01.

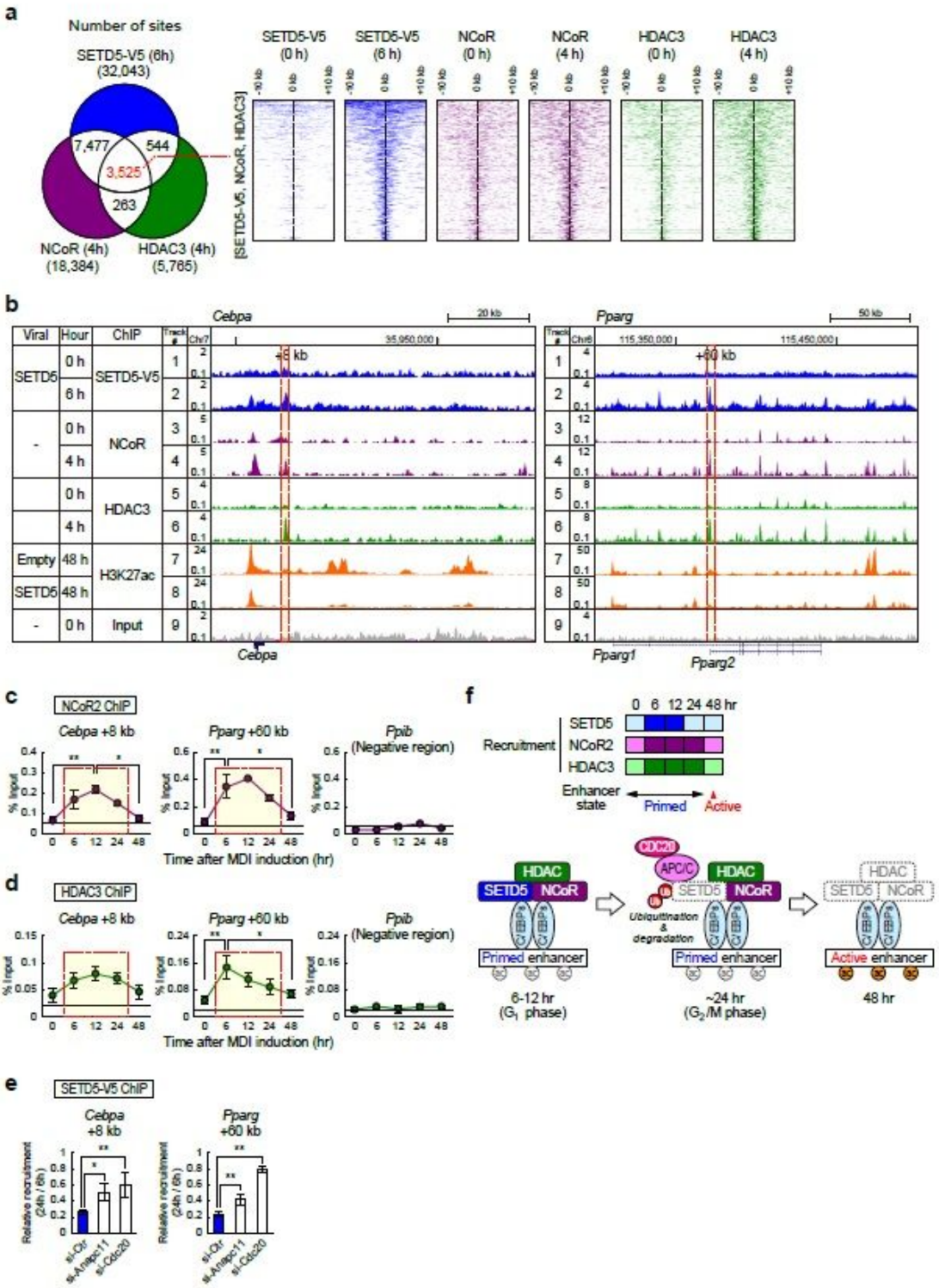

Figure 5

SETD5 is co-recruited to primed enhancers with NCoR-HDAC3 complex and diminishes prior to enhancer activation. a Venn diagram (left) and heatmap (right) representation of genomic regions occupied by SETD5-V5, NCoR, and HDAC3. Approximately 60% of NCoR and 71% of HDAC3 genomic binding regions were co-occupied by SETD5-V5. Heatmap analysis showing ChIP-seq data for SETD5-V5, NCoR, and HDAC3 at a 20-kb region centered on SETD5-V5 binding region. ChIP-seq data for NCoR and HDAC3 were

from the previously published paper 32. b Genome browser representation for SETD5-V5, NCoR, HDAC3 and H3K27ac on Cebpa and Pparg genes in 3T3-L1 preadipocytes. Tracks 1-2 and 7-9 are the same data as Fig. 4c. ChIP-seq for NCoR and HDAC3 was from the previously published paper 32. c, d ChIP-qPCR analyses of NCoR2 (c) and HDAC3 (c) on Cebpa and Pparg genes during the early adipogenesis. 3T3-L1 preadipocytes transduced with control empty virus were subjected to ChIP-qPCR analyses using anti-NCoR2 or anti-HDAC3 antibody. Data are represented as mean ± SEM of three to four independent experiments. Statistical test was performed for comparisons of group (Tukey's post hoc comparison). *p<0.05; **p<0.01. e ChIP-qPCR analysis of SETD5-V5 on Cebpa and Pparg genes under knockdown of ANAPC11 or CDC20. 3T3-L1 preadipocytes transduced with SETD5-V5 were transfected with control siRNA or siRNA targeting to Anapc11 or Cdc20 and subjected to ChIP qPCR analysis at 6 hr and 24 hr of differentiation using anti-V5 antibody. ChIP signal was presented as relative SETD5- recruitment. Error bars represent mean ± SD of three technical replicates. Statistical test was performed for comparisons of groups (Tukey's post hoc comparison). *p<0.05, **p<0.01. f Schematic model of SETD5-NCoR-HDAC3 complex formation and the loss of SETD5 on enhancers during transition from primed to active states. Heatmap shows degree of recruitment of SETD5, NCoR2, and HDAC3 to Cebpa and Pparg enhancers (based on Fig. 4d, 5c, and 5d). Darker color indicates more recruitment.

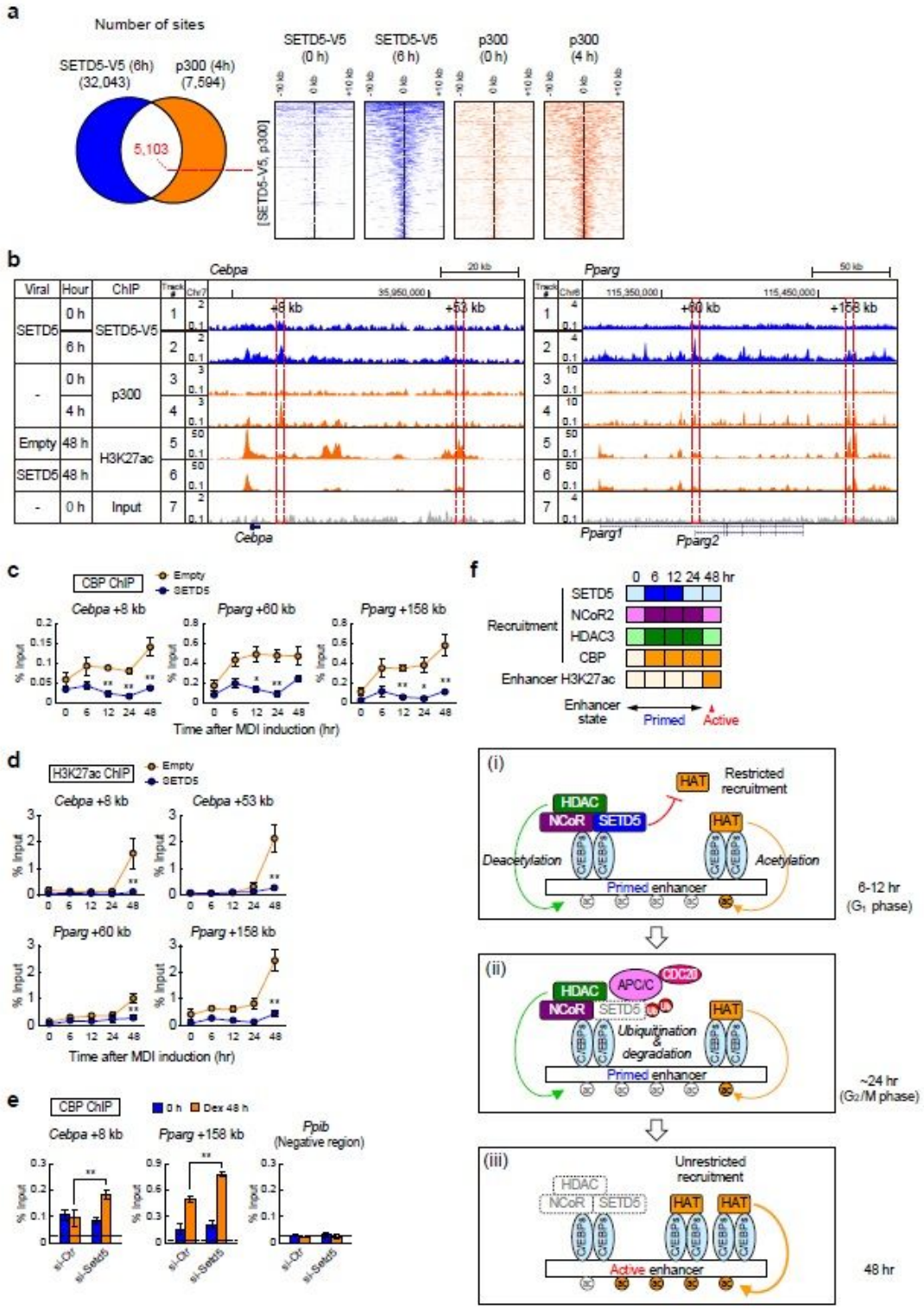

Figure 6

SETD5-NCoR-HDAC3 complex restricts HATs recruitment to primed enhancers. a Venn diagram (left) and heatmap (right) representation of genomic regions occupied by SETD5-V5 and p300. Approximately 64% of p300 genomic binding regions were co-occupied by SETD5-V5. Heatmap analysis showing ChIP-seq data for SETD5-V5 and p300 at a 20- kb region centered on SETD5-V5 binding region. ChIP-seq data for p300 were from the previously published paper 32. b Genome browser representation for SETD5-V5,

p300, and H3K27ac on Cebpa and Pparg genes in 3T3-L1 preadipocytes. Tracks 1-2 and 5-7 are the same data as Fig. 5b. ChIP-seq for p300 was from the previously published paper 32. c, d ChIP-qPCR analyses of CBP (c) and H3K27ac (d) on Cebpa and Pparg genes during the early adipogenesis. 3T3-L1 preadipocytes transduced with control empty virus or SETD5 were subjected to ChIP-qPCR analyses using anti-CBP or anti-H3K27ac antibody. Data are represented as mean ± SEM of three to five independent experiments. Statistical tests for ChIP-qPCR of CBP and H3K27ac were performed for two sets of data (Student's t-test) and comparisons of group (Tukey's post hoc comparison), respectively. *p<0.05; **p<0.01. e ChIP-qPCR analysis of CBP on Cebpa and Pparg enhancers during adipogenesis. 3T3-L1 preadipocytes transfected with siRNA targeted to Setd5 were subjected to ChIP-qPCR analysis of CBP at indicated time after Dex induction of differentiation. The experiments were performed twice, and the representative one is shown. Error bars represent mean ± SD of three technical replicates. Statistical test was performed for comparisons of group (Tukey's post hoc comparison). **p<0.01. f Model of enhancer transition from primed to active state during adipogenesis. Heatmap shows degree of recruitment of SETD5, NCoR2, HDAC3, and CBP to Cebpa and Pparg enhancers and H3K27 acetylation (based on Fig. 4d, 5c, 5d, 6c, 6d, Supplementary Fig. 1d). Darker color indicates more recruitment and acetylation. (i) SETD5 forms a complex with NCoR-HDAC3 and keeps a hypoacetylation state by restricting the recruitment of HAT to primed enhancers. (ii) SETD5 in NCoR-HDAC complex on primed enhancers is ubiquitinated and degraded by APC/C. (iii) Degradation of SETD5 from NCoRHDAC3 co-repressor complex allows the unrestricted recruitment of HAT and H3K27 acetylation and transit enhancers from primed to active state.

Supplementary Files

This is a list of supplementary files associated with this preprint. Click to download.

- 021621NCSupplementaryFigures.pdf